CHAOS IN NUMERICAL SOLUTION OF DYNAMICAL SYSTEMS

BY

PADMA JAGANNATHAN

DEPARTMENT OF MATHEMATICS

SCHOOL OF PHYSICAL SCIENCES

SUBMITTED

IN

PARTIAL-FULFILMENT OF THE REQUIREMENT FOR THE DEGREE OF

MASTER OF PHILOSOPHY

To

THE NORTH-EASTERN HILL UNIVERSITY

SHILLONG

DECEMBER, 1983

DS
515.35
JAG

[redacted]
Acc. no. 102927
Acc by [redacted]
Date 26-2-98
Class by [redacted] 15/7/1400
Sub Heading by [redacted]
Enter by [redacted]
Transcribed by [redacted]

TO MY UNCLE

T.S.SRINIVASAN

Phone : 6945
Grams : NEHU

North - Eastern Hill University

DEPARTMENT OF MATHEMATICS

Bijni Campus
Bhaggyakul
Shillong-793003.

CERTIFICATE

I certify that the dissertation entitled "Chaos in Numerical Solution of Dynamical Systems" submitted by Miss. Padma Jagannathan in partial fulfilment of the requirements for the degree of Master of Philosophy is the outcome of a study undertaken by the candidate.

I certify that the sources from which ideas have been borrowed have been duly reffered to.

The material in this dissertation has not been presented for award of a degree in any university before.

This dissertation may be placed before the examiners for evaluation and necessary formalities. I certify that this dissertation is worthy of consideration by the examiners.

13/12/83

Y.S.T.RAO

Advisor

School of Physical Sciences

North Eastern Hill University

S H I L L O N G.

Details of the courses cleared by Miss Padma Jagannathan for the M.Phil course.

COMPUTER PROGRAMMING	70%
NUMERICAL ANALYSIS	85%
TOPOLOGY	71%
FRENCH	85%

Average grade point is 5.2 (GRADE - 'A')

13-12-83

ACKNOWLEDGEMENTS

I am highly indebted to Dr. Y.S.T. Rao for the guidance and encouragement he has given.

I am grateful to Dr. S.S. Khare, Head, Department of Mathematics for his keen interest and help extended by him.

I also thank Shri Pradip Dey for typing this thesis at short notice.

Discussions with Prof. N. Dev and Prof. H.K. Mukherjee were also very useful. I thank them all.

CONTENTS

*****

CHAPTER - I

INTRODUCTION

1.1 : Dynamical System :

Dynamical systems were evolved during the study of ordinary differential equations in the late 19th Century. These can be either continuously evolving systems such as planatory motion etc., or discrete systems. The continuous evolution of systems with time led to the study of ordinary differential equations.

Till recently it was generally believed that most systems with a few degrees of freedom behaved in a very orderly manner, i.e., given a certain set of accurate initial conditions, the future or the past could be predicted accurately.

This confidence in such causal connection between the states of a system at two infinitesmally separated time-instants led to the extensive use of the theory of differential equations in the so called exact sciences.

In the 19th Century with development of Kinetic theory the concept of causality and irreversibility got

blurred when dealing with large systems which led to ergodic theorems etc.

1.2 : Chaos in Dynamical Systems :

Recent studies have discovered that even systems with a few degrees of freedom behaved erratically, i.e., given any set of boundary conditions the behaviour of the system at any given time cannot be predicted reliably, whereas the so-called 'normal' systems have closed orbits or such regular trajectories, these systems would behave in an apparently chaotic manner. In such a case the system is said to behave chaotically. Any two system initially close to each other after a certain interval of time can change as much as permitted by the conservation laws. Similarly some typical orderly systems may approach a particular point and stay there once they reach the point (such a point is called an attractor).

For certain systems the set of attractors is uncountable and has fractional dimension and what is more, the system jumps from one point to another in the set covering almost all points in the set.

1.3 : Plan of our Presentation :

In this work, we discuss chaotic motion of dynamical systems near strange attractors.

In the remainder of this chapter, we introduce ordered dynamical systems to lay the foundation for the chapters to come.

In chapter II, we discuss the chaotic behaviour of some dynamical systems near strange attractors.

In chapter III we re-examine, in detail, the logistic equation in the Central Difference Scheme as studied by Yamaguti and Ushiki.

Chapter IV simulates strange attractors through the composition of two simple harmonic motions in mutually perpendicular directions.

1.4 : Ordered Dynamical Systems :

A dynamical system is a way of describing the motion of a certain set of points in a space in course of time. It is a set of solution-curves of differential equation.

A system of differential equations :

$$\dot{u}_i = f_i(u_1, u_2, \cdots, u_n), \; i = 1, 2, \cdots, n, \quad \cdots (1.1)$$

where f_i's do not depend on t is called autonomous. The space of the variables u_i, $i = 1, \cdots, n$, is called the Phase Space. The solution of equations 1.1 in the phase space is called a trajectory with the boundary conditions $\underline{u}(t=0)=\underline{u}_0$.

From the same set of equations, it follows that the trajectories do not intersect. A trajectory consisting of a single point $\underline{u}_0$ is called a rest point (fixed point, stationary point or equilibrium point). Then

$$\underline{f}(\underline{u}_0) = 0 \qquad \ldots (1.2)$$

Every point of the phase space belongs to exactly one trajectory except for fixed points.

To illustrate some simpler aspects, we consider a system in R_2 :

$$\frac{du}{dt} = P(u,v)$$
$$\frac{dv}{dt} = Q(u,v) \qquad \ldots (1.3)$$

P and Q have continuous first order partial derivatives in the neighbourhood of (u_0, v_0) where,

$$P(u_0, v_0) = 0$$
$$Q(u_0, v_0) = 0 \qquad \ldots (1.4)$$

Then (u_0, v_0) is called a fixed point or critical point. A critical point (u_0, v_0) of the system is called isolated if there exists an open neighbourhood of it wherein (u_0, v_0) is the only critical point. If P, Q are differentiable at that point, in the neighbourhood of (u_0, v_0) we can rewrite 1.4 as

$$\dot{\underline{r}} = \underline{\underline{A}}\,\underline{r} + \text{higher order terms.} \qquad \ldots (1.5)$$

where

$$r_1 = u - u_0 \qquad \ldots(1.6)$$
$$r_2 = v - v_0$$

where $\underline{A}$ is a real 2 x 2 matrix. If $\underline{A}$ is non-degenerate (det $\underline{A} \neq 0$), we can select small enough neighbourhoods where one could neglect higher order terms. Making a time independent, invertible linear transformation

$$\underline{r} = \underline{T}\,\underline{r}'$$

in the uv-plane we get

$$\frac{d\underline{r}'}{dt} = \left(\underline{T}^{-1}\underline{A}\,\underline{T}\right)\underline{r}' \qquad \ldots(1.7)$$

By a proper choice of $\underline{T}$, $\underline{T}^{-1}\,\underline{A}\underline{T}$ can be brought into canonical form with diagonal elements λ_1, λ_2 : λ_1, λ_2 being the eigenvalues of the matrix $\underline{A}$.

Without any loss of generality, we consider the origin C, (o,o), to be the critical point. Then several cases are of interest.

Case I : We first consider the situation where the eigenvalues are real.

(a) $\lambda_1 < \lambda_2 < 0$.

All systems starting in the neighbourhood of C converge to it. Such a point is called a stable node. This is also called an attractor. (Fig. 1.1a)

(b) $\lambda_1 > \lambda_2 > 0$.

Here also C is a node but the systems starting from a small neighbourhood of C diverge away from C. Such a point is called a repellor. The qualitative picture in this case is shewn in Fig. 1.1a with the arrows reversed.

(c) $\lambda_1 < 0 < \lambda_2$.

Almost all the trajectories (with very few exceptions) in the neighbourhood of the critical point have the form of hyperbolae. Here none of the non-rectilinear paths approach C as $t \to +\infty$ or $t \to -\infty$. Here only two half lines passes through the origin. Then C is called an unstable saddle point (Fig. 1.1b)

(d)(i) $\lambda_1 = \lambda_2 < 0$.

Here C is called a node. If A is diagonisable then the trajectories are straight lines approaching C. Then C is a stable node. (Fig 1.1c).

In case A is not diagonisable the trajectories are curved paths approaching C (Fig. 1.1d). Here C acts as an attractor.

(ii) $\lambda_1 = \lambda_2 > 0$.

This is the same as the above situation, but

here C acts as a repellor (see Fig. 1.1c and Fig. 1.1d with arrows reversed).

Case II : Now we consider situations with the eigenvalues(λ) complex.

Then three cases arise:

(a) $Re\,\lambda < 0$.

Here the paths approache C in a spiral path. Then C is called a stable spiral point (Fig 1.2a)

(b) $Re\,\lambda > 0$.

The situation here is the same as above except that the paths approach C as $t \to -\infty$ (see Fig 1.2 a with arrows reversed). This critical point is an unstable spiral point.

(c) $Re\,\lambda = 0$.

Here C is surrounded by an infinite family of closed paths but it is not approached by any path. Then C is stable and is called a center. (Fig. 1.2 b)

This behaviour can be illustrated easily if instead of a continuous development through a set of differential equations, if one considers a discrete time steps h so that the time evolution can be considered to be an iterated map

$$X[(n+1)h] = F[X(nh)] \qquad \ldots (1.8)$$

The point Xo such that $F(X_o) = X_o$ will be a fixed point and if $|\partial F/\partial x| < 1$ then X_o will be an attractor in the above sense. This form of description will be used more often in the chapters to come.

The behaviour of the trajectories may change drastically if equations 1.3 are non-linear. This will be discussed in the next chapter.

CHAPTER - II

STRANGE ATTRACTORS AND CHAOS

2.1 : Introduction

In the previous chapter we had discussed various types of fixed points and attractors in normal systems. We had a situation where the set of fixed points was a singleton.

Now we consider the cases where the behaviour of the system is erratic near the attractors. Consider a map T on a compact set X, satisfying the following conditions.

(i) X is invariant under T, i.e.,

$$TX = X ,$$

(ii) X has a shrinking neighbourhood i.e. there exists an open neighbourhood U of X, $U \supset X$, such that

$TU \subset U$.

Then X is called an attractor.

(Eckmann 1983, Ott 1981)

On the other hand the system may not have any points which are attractors but it may have two distinct points say P_1, P_2 such that under an iterated map F a

neighbourhood N_1 of P_1 gets mapped into a neighbourhood N_2 of P_2 and in turn N_2 gets mapped into N_1. Then under F^2 ($\equiv F.F$), N_1 (or N_2) gets mapped into N_1 (or N_2) itself. If F is a contracting map then $|\det(\underline{F}/X)| < 1$. However, neither of P_1, P_2 are fixed points (as $F(P_k) \neq P_k$, $k = 1, 2$.). But if the system starts from neighbourhoods of P_1 or P_2 it converges to a two-point cycle. Now if F is parametrized by some parameter say α, then a change in the parameter α may make the two-point cycle unstable and may generate a four-point stable cycle which in turn, in course of time may generate 2^3, 2^4, ..., 2^n- point cycles. When the parameter α takes a certain value a 2^∞- point cycle may be generated. This set of points is uncountable and will be called a strange attractor. This behaviour may continue for further increase of α and later a stable 3-point and other stable cycles may be generated.

The importance of strange attractors follows from the fact that the system is confined to an uncountably infinite set of points and moves in an apparently erratic manner but does not fill any sizable volume of the phase space. In particular the phase space has fractional dimensions. Now we discuss a few examples of strange attractors from literature.

2.2 <u>Hénon-Heiles Oscillator</u> :

We begin to illustrate the concepts of chaotic

behaviour near strange attractors by summarizing the work of Hénon-Heiles. They studied a dynamical system of two degrees of freedom given by the Hamiltonian e.g. (Joseph Ford 1983)

$$H = \frac{1}{2}(p_1^2 + q_1^2 + p_2^2 + q_2^2) + q_1^2 q_2 - 1/3\, q_2^3 \qquad \ldots(2.1)$$

They obtained numerical solutions for the equations describing the trajectories of the system for several energies. For sufficiently small energies the cubic terms have marginal effect and the qualitative description of the motion can be understood by approximating the motion through two uncoupled simple harmonic motions of same periods. The phase space is four dimensional. Besides the Hamiltonian H, we can also have $H_1 (= \frac{1}{2}(P_1^2 + q_1^2))$ as a constant of motion. Thus there are two constants of motions and so the trajectory is confined to a two dimensional surface. The intersection of these trajectories with any arbitrary plane gives closed orbits. For example, when the cubic terms are neglected, these intersections (also called Poincare maps) in the (p_2, q_2) plane is a circle. But with larger energies the influence of the cubic terms becomes important and H_1 is no longer a constant of motion even approximately. Then we have only one constant of motion which is H itself. Therefore the trajectories will no longer be confined to 2- dimensional surfaces but can roam around

in a 3-dimensional manifold. Such a trajectory will intersect an arbitrary plane at discrete set of points.

For small energies where there were two constants of motion, they found that at the energy level E = 1/12 the intersections of the trajectories with the (q_2, p_2) plane were closed orbits and hence the motion is orderly. But as the energy is increased the motion gets turbulent and the intersection of these trajectories with the plane results in points where the trajectory enters the plane from one direction and then comes back through a second point. Thus for an energy exceeding E=1/12 and less than E = 1/8, sometimes the trajectories are confined to a 2-dimensional manifold and sometimes to a 3-dimensional manifold. So at these energy levels some of the orbits are still closed whereas some of them generate scattered points. But with still larger energies there are no 2-dimensional manifolds and the motion is completely chaotic. A single trajectory would cross a given (q_2, p_2) plane infinite number of times, through countably infinite discrete set of points, but not through closed orbits. Two orbits which start with almost identical initial boundary conditions could in course of time separate out to the maximal extent possible and the motion gets turbulent. Around E = 1/12, points initially close to each

other separate linearly in course of time, whereas near E = 1/6, they separate exponentially.

Thus the transition of the orbital motion from a two dimensional to a three-dimensional surface introduces chaos in the motion.

2.3 : Iterated Model

Consider the non-invertible map : (Joseph Ford 1983).

$$X_{n+1} = 2X_n \text{ (Mod 1)} \qquad \ldots (2.2)$$

The solution of equation 2.2 is :

$$X_n = 2^n X_0 \text{ (Mod 1)} \qquad \ldots (2.3)$$

Suppose X_0 is written in binary representation :

$$X_0 = 0.\ 110000\ 111\ 0\ 1111 \qquad \ldots (2.4)$$

then the iterated maps of equation 2.2 are generated by moving the decimal point sequentially to the right and dropping the integer part. All the iterates of X_0 lie on the unit interval (0.1). Let this interval be partitioned into two cells viz., the left cell ($0 \leq x < \frac{1}{2}$) and the right cell ($\frac{1}{2} \leq x < 1$). A given iterate X_n is in one of these two cells as its first digit is zero or one. Since in general, the future digits of X_0 cannot be determined from any past finite part of the digits of X_0, the true

orbits are chaotic. This is true even when we take any finite number of equal partitions of (0,1) instead of just two.

In case now, instead of finite partitions, infinite partitions having zero cell size are taken, then a cell number sequence is just the precise X_n sequence itself. If the cell number digit string of an orbit is random, then the orbit itself is chaotic.

2.4 : One-dimensional non-invertible maps

In order to understand chaos from a much simplified model we consider one-dimensional non-invertible maps instead of complicated differential equations.

Consider the sequence $x_0, x_1, x_2, \ldots\ldots\ldots$, generated by the map F. Let the sequence be bounded. This is possible if the sequence depends on the choice of the initial values. The average correlation function between two members separated by m steps may go to zero as $m \to \infty$, and the sequence may become non-periodic. The behaviour of such an iterated map is called chaotic and is usually observed in case where the map is non-invertible. Quite often it corresponds to a magnification or elongation and a folding of the trajectory.

Two special examples of non-invertible maps are (Ott 1981; Bambi Hu 1982)

$$F_1(x) = a(1 - 2\,|x - \tfrac{1}{2}|), \quad 0 < a \leq 1 \quad \ldots (2.5)$$

$$F_2(x) = 4bx\,(1-x), \quad 0 < b \leq 1 \quad \ldots (2.6)$$

where a and b are constants. Qualitatively both these maps are similar in the sense that they describe a single peaked curve and the first map (F_1) has a sharp corner whereas the second map (F_2) has a smooth maximum. Consequently the second mapping has been used more often.

For $0 < b < 1$, F_2 maps the unit interval into itself. The line $x_n = x_{n+1}$ intersects this map at $x_n = 0$ and $x_n = x^* = 1 - 1/4b$ for $1/2 < b < 1$. These points of intersection are the fixed points of the map.

$$F'(0) = 4b$$

$$F'(x^*) = 2(1 - 2b)$$

In the region $0 < b < 1/4$, the origin is a stable fixed point. For $1/4 < b < 3/4$, F_2 converges to x^*. In this region x^* is stable whereas the origin becomes unstable. But for $3/4 < b < 1$, both the origin and x^* are unstable. When x^* becomes unstable (b just exceeds $3/4$) it generates a stable two-point cycle, say, e,f, such that F(e)=f, F(f)=e.

When b is furtherincreased this two-point cycle looses its stability and around b=0.862.. a four-point cycle is generated followed by 8, 16, 32, etc point cycles.

The range of values over which a 2^k-point cycle is stable decreases geometrically with k and b approaches 0.892 as $k \longrightarrow \infty$. The uncountable set of points got when $k \longrightarrow \infty$ will be called a strange attractor. Beyond the value of b = 0.892 the system behaves chaotically. A further increase in b will lead to the emergence of a three-point cycle and other cycles. In fact Li, T - Y, and J.A. Yorke (1975) have proved that a three-point cycle implies chaos.

2.5 : Two-Dimensional Invertible Maps

A noninvertible one-dimensional map discussed above can be written as a two dimensional invertible map as follows :

$$x_{n+1} = F(x_n) + y_n$$
$$y_{n+1} = b\, x_n \qquad \ldots (2.7)$$

where F(x) is noninvertible. If $b \neq 0$ then $x_n = y_{n+1}/b$ and $y_n = x_{n+1} - F(y_{n+1}/b)$. (Ott 1981; Bambi Hu 1982).

For a very small b, equation 2.7 can be considered as a one-dimensional noninvertible map.

The Jacobian of the transformation is :

$$J = \begin{vmatrix} \frac{\partial x_{n+1}}{\partial x_n} & \frac{\partial x_{n+1}}{\partial y_n} \\ \frac{\partial y_{n+1}}{\partial x_n} & \frac{\partial y_{n+1}}{\partial y_n} \end{vmatrix} = -b \, .$$

If $|b| < 1$, the areas will contract by a factor of $|b|$ on each application of the map 2.7. Then a square of unit area about the origin under the above mapping successively decreases in area and asymptotically approaches a subset with zero area in the xy-plane. This subset is an attractor. This subset would have dimension less than two.

Now consider a set in an n-dimensional space and partition it into a number of cubes of side ε . Let $N(\varepsilon)$ be the number of cubes needed to cover the set. Then the dimension (d) of the set is difined by :

$$d = \lim_{\varepsilon \to 0} \frac{\ln N(\varepsilon)}{\ln (1/\varepsilon)} \qquad \cdots (2.8)$$

If an attractor has a fractional dimension then it is called a strange attractor.

Hénon studied the following mapping :

$$x_{n+1} = 1 - a x_n^2 + y_n$$
$$y_{n+1} = b\, x_n \qquad (2.9)$$

In this case

$$J = \begin{vmatrix} -2ax_n & 1 \\ b & 0 \end{vmatrix} = -b$$

He used the initial conditions $x_0 = 0.631$ and $y_0 = 0.189$ with $a = 1.4$ and $b = 0.3$. Under repeated iterated mapping

millions of times, a bulk of the points would lie very near the attractor. The points are well distributed throughout the attractor. This distribution is independent of the starting point, provided it is in the basin of attraction which is a quadrilateral with ABCD defined by A = (- 1.33, 0.42) B = (1.32, 0.133), C = (1.245, -0.14) and D = (-1.06, -0.5). The attractor broadly speaking has a shape of a parabola. To see this consider equation 2.9 with small values of b. Then we have

$$x_{n+1} = 1 - a\left(\frac{y_{n+1}}{b}\right)^2 + y_n \qquad \cdots (2.10)$$

Since a = 1.4, for small b, one can approximate the above equation to :

$$x_{n+1} = 1 - \frac{a}{b^2} y_{n+1}^2 \qquad \cdots (2.11)$$

The mapping has two fixed points P_1=(0.631544, 0.1894063) and P_2 = (- 1.1313544, -0.3394063). A peculiar behaviour of the attractor near P_1 is noticed. If one considers a small square S_1 of side 0.1 about P_1, and magnify it and then again take a smaller square S_2 of side 0.01 about P_1, then the distribution of points in S_2 looks quite similar to that in S_1. This phenomenon was shown to continue for about 3 stages of successive magnifications. However, to see even the third magnification he needed a few million iterations.

We give a much simpler explanation of this feature of the attractor now. In particular we consider the self-similarity property of the attractor under scale-invariance. For this consider the transformation of an infinitesmal line element (dx, dy) near (x,y). It is transformed under the map in equation 2.9 to (dx', dy').

$$\begin{pmatrix} dx' \\ dy' \end{pmatrix} = \begin{pmatrix} -2.8x & 1 \\ 0.3 & 0 \end{pmatrix} \begin{pmatrix} dx \\ dy \end{pmatrix}$$

The eigenvalues of the above matrix T are :

$$\lambda_1 = -1.4\,x + \sqrt{1.96x^2 + 0.3} \quad \text{and}$$
$$\lambda_2 = -1.4\,x - \sqrt{1.96x^2 + 0.3}.$$

such that $\lambda_1\lambda_2 = -0.3$. Then magnitude of one of them is less than 0.55 ($= \sqrt{0.3}$) (say λ_s) while that of the other is always greater than $\sqrt{0.3}$. In fact the larger eigenvalue (λ_L) exceeds 1.0 if $|x| > 0.25$ (see table 2.1). Let the corresponding eigenvectors be ξ_2 and ξ_1. Then any arbitrary vector $d\xi$ can be expressed as a linear combination of ξ_1 and ξ_2. If $|x| > 0.25$, $|\lambda_L|$ exceeds 1 and $|\lambda_s| < 0.3$, one can consider a square enclosed by $\varepsilon\xi_1$ and $\varepsilon\xi_2$ where $\varepsilon \ll 1$. This square gets mapped into a rectangle with the larger side $\varepsilon|\lambda_L|$ and the smaller side $\varepsilon|\lambda_s|$. Thus under repeated maps one expects

this square to degenerate to a line of infinite length. Therefore the attractor has dimension at least one. But as the line of infinite length is, confined to the basin of attraction, it gets folded. In fact if we consider the parabola of equation 2.11, under the map it gets folded once and looks like two parabolae joined at one end. A repeated map will generate four parabolae linked successively. This process continues ad. infinitum. In this process the attractor set is of dimension 1.26.

Now consider a small line segment A_1B_1 near P_1 in the ξ_1 direction with P_1O_1 lying in the ξ_2 direction where O_1 is the centre of A_1B_1. Then under the mapping A_1B_1 gets magnified by a factor of 1.92 ($|\lambda_1|$ near x=0.6315) with direction being reversed and with its centre O_2 such that O_2P_2 lies along the ξ_2 direction but with the distance O_1P_1 contracted by a factor of 0.156 ($|\lambda_2|$ near x = 0.6318) (See Fig 2.1). Another iteration of A_2B_2 gives us A_3B_3 with O_3P_1, 0.156 times O_2P_1 and A_3B_3 twice of A_2B_2. Thus under successive mappings the points on the line element initially close to each other get separated and successive iterations of such small line segments in different magnifications show similar properties. Thus the set acts as an attractor which is called the Hénon's attractor.

CHAPTER III

CHAOS IN CENTRAL DIFFERENCE SCHEME FOR LOGISTIC EQUATION

3.1 : Introduction :

Yamaguti and Ushiki (1981) have considered a simple Ordinary Differential Equation that exhibits chaotic behaviour when solved numerically. In this chapter, we consider their problem and give an alternate and simpler explanation for the behaviour of the system.

They considered the ordinary differential equation :

$$\frac{dy}{dt} = y(1-y), \qquad \cdots (3.1)$$

with initial condition $y(0) = y_0$, $(0 < y_0 < 1)$.
A direct integration gives :

$$y = \frac{1}{1 + c\, e^{-t}} \qquad (3.2)$$

where

$$c = \frac{y_0}{1 - y_0}$$

The exact solution starting from $0 < y_0 < 1$ is monotonically increasing and converges to 1 as $t \to +\infty$ Here y=1 is the saturation point.

A physical representation of equation 3.1 is the growth of the population. If u is the population at a certain time then du/dt is the rate of growth of the population. The rate of growth is proportional to the present population and the mutual destruction is proportional to the square of the population. After a certain time, the population reaches a saturation point and remains constant. After proper scaling of population and time, the system is well represented by equation 3.1 .

3.2: Central Difference Scheme

If the integration is to be done numerically the simplest method to use would be

$$u\{(n+1)h\} = u(nh) + h\left(\frac{du}{dt}\right)_{nh} + O(h^2)$$

However, since $u\{(n-1)h\}$ is already available

$$u\{(n+1)h\} = u\{(n-1)h\} + 2h\left(\frac{du}{dt}\right)_{nh} + 2h^3\left(\frac{d^3u}{dt^3}\right)_{nh} + O(h^5)$$

is a better approximation and is expected to yield a more accurate result.

Physically, this implies that the rate of

production depends on the level of the species at an earlier time in addition to the present population level, thus simulating the delay in the production mechanism.

Now if equation 3.1 were to be solved by the Central Difference Scheme.

$$\frac{u_{n+1} - u_{n-1}}{2h} = u_n(1 - u_n) \qquad \ldots\ (3.3)$$

with two initial conditions $u_0 = y_0$ and $u_1 = Y_0 + h\,Y_0(1 - Y_0)$, (where u_1 is evaluated to a three digit accuracy), then the solution behaves peculiarly.

With $y_0 = 0.5$, $u_1 = 0.525$ and with step size $h = 0.1$, the equation 3.3 gives an unstable phenomena. These types of solutions are called ghost solutions.

From their calculations on a calculator with single precision and with the above mentioned initial conditions, they found that for $0 < t < 8.6$, the numerical solution gives a good approximation of the true solution. In this region the solution u_n increases monotonically and approaches 1.0. But for $t > 8.6$ the monotonocity is lost and the solution starts zig-zagging. When $t = 9.7$, the value of u_n crosses 1.0 for the first time and the solution begins to oscillate. The growth of the amplitude of oscillation is geometric.

and its rate of growth is such that the amplitude is multiplied by about e = 2.71.... for $\Delta t = 1.0$. Around t = 17.0, the oscillation looses its symmetry with respect to y = 1.0. At t = 19.6, u_n takes a negative value for the first time. The maximal values reach 1.5 and then start decreasing. The smaller values go down to -0.5 and then both approach 0.0 while oscillating. At t = 33.8, u_n exceeds 0.5 and it recovers the values u_n and u_{n+1} almost identical to the initial conditions u_0 and u_1 and the cycle begins again.

The ghost solutions appear even if h is very small. One of the reasons put forward by them is that the Central Difference Scheme is a second order difference scheme and instability enters at y = 1.0 and y = 0.0. They deduced that the global behaviour of the numerical solution computed by the Central Difference Scheme is very sensitive to the initial condition, time-mesh length and the precision of the computer employed. In a computer with single or double precision the cycle was repeated more than 10^5 times. But with quadruple precision it diverged to $-\infty$ after two cycles. The solution when calculated using a simple programmable calculator diverged to $-\infty$ after one cycle itself. They also observed that the time needed for one cycle depends on the precision used and that the period of stay is approximately proportional to the order of precision. They attributed

the phenomenon to the round-off errors.

3.3: Our Numerical Results

In order to study their results we simulated our machine to act as a 2,3,4,5,6,7,8 and 9 digit machine and we also made it act like a round-off machine for different step sizes and initial values. In general all the cases except for a few (which we discuss later), follow a similar pattern.

The Central Difference Scheme represented by Equations 3.3 can be rewritten as set of coupled first order finite difference equations.

$$u_{2n+2} - u_{2n} = 2h\, u_{2n+1}(1 - u_{2n+1}) \quad \ldots(a)$$
$$u_{2n+1} - u_{2n-1} = 2h\, u_{2n}(1 - u_{2n}) \quad \ldots(b) \qquad (3.4)$$

For simplicity we denote u_{2n} by u and u_{2n+1} by V_n so that equation 3.4 becomes

$$u_{n+1} - u_n = 2h\, v_n(1 - v_n) \quad \ldots(a)$$
$$v_{n+1} - v_n = 2h\, u_n(1 - u_n) \quad \ldots(b) \qquad (3.5)$$

For a small time step, u_n and v_n keep increasing monotonically between the initial value and 1.0. But when the value of u_n reaches 0.9934, then the value of v_n is slightly lower and the zig-zagging starts at this point. Once the value of u_n just exceeds $1-5\epsilon$ where ϵ is the least count of the machine, then v_n does not

gain at all. So consecutive v_n values remain the same provided $u_n < 1.+5\varepsilon$ This continues till u_n exceeds $1. + 5\varepsilon$. Then onwards u_n keeps increasing as its derivative is positive, whereas that of v_n being negative, its value starts decreasing. u_n reaches its maximum value 1.5 when v_n reaches 0.0, (as the R.H.S. of equation 3.5(a) vanishes for v_n=0.0) after which it starts decreasing. Now both u_n and v_n keep decreasing till v_n reaches its lowest value -0.5 (as R.H.S. of equation 3.5(b) vanishes for u_n=1.0). Then onwards it starts increasing trying to reach the value zero. At the same time u_n also approaches zero. When $u_n \ll 1.$ then $v_n \approx - u_n$. Here any one of u_n or v_n may attain a value whose magnitude is less than 5ε first.

Suppose u_n attains this value first. In this case v_n does not get any lift and so it remains unchanged till u_n reaches -5ε . After that both u_n and v_n tend to $-\infty$. But this occured only in three cases when we simulated the machine to a 2,4 and 5 digits truncating machine.

On the other hand in case v_n attains a value slightly greater than -5ε first, then u_n does not get any help at all and so remains unchanged till v_n attains a value slightly greater than 5ε. After v_n crosses the 5ε mark both u_n and v_n start increasing in the positive

direction and another cycle starts. These results are independent of precision, step-size and initial value. Two examples of this behaviour are shown in Fig 3.2 and Fig 3.3. Whereas in the case of 6 digit accuracy v reaches zero earlier and then onwards the next cycle starts (Fig 3.2), in the case of 5 digit calculation u approaches zero first, after which both u, v tend to $-\infty$ (Fig 3.3)

The initial values we used were u_0=0.5 and u_1=0.5249791874 (calculated exactly from equation 3.2). Using these initial values and time step h = 0.1, we found that zig-zag started at t=5.0, and u_n reached a value just greater than 1.0 when t=6.5. After that till t=20.3, the chaos continued, at which point u_n approached zero. The duration of chaos is seen to be independent of precision, change in initial value, truncation or rounding.

3.4: Analytical Explanation

If v_n is calculated from equation 3.2, the non-chaotic region is more or less independent of accuracy, step-size, initial value, precision, etc. On the other hand if u_n is fed only to three digit accuracy, additional error (say positive) introduced in v_n would supress u_n, which in turn would enhance v_n and this may cause additional complications. Equations 3.5 are a finite difference

representation of a set of two coupled first order differential equations (if we neglect terms of the order of h^3)

$$\frac{du}{dt} = v(1-v) \quad \cdots(a)$$
$$\frac{dv}{dt} = u(1-u) \quad \cdots(b) \qquad (3.6)$$

where we denote even values by u and odd values by v. The initial boundary conditions would give values of u and v at t=0.

Now eliminating time from equations (3.6) gives us

$$\frac{du}{dv} = \frac{v(1-v)}{u(1-u)} \quad \cdots\cdots (3.7)$$

A straight forward integration gives us

$$\frac{1}{2}u^2 - \frac{1}{3}u^3 = \frac{1}{2}v^2 - \frac{1}{3}v^3 \quad \cdots (3.8)$$

where the integrating constant is kept zero as u and v coincide in the non-chaotic region. Equation 3.8 can be regarded as a cubic equation for v in terms of u. Solving this equation gives us :

$$v = u \quad \cdots(a)$$
$$v = \frac{(3-2u) \pm \left[(3-2u)^2 + 8u(3-2u)\right]^{1/2}}{4} \quad \cdots(b) \qquad (3.9)$$

The first root 3.9(a) corresponds to normal behaviour. The solution in this case is given by

$$u = v = \frac{1}{1+Ce^{-t}} \quad \cdots (3.10)$$

Now, in equation 3.9(b) we choose the upper sign (plus).

This will give us v as the upper branch and u as the lower branch in Fig 3.1 during chaos.

A change of dependent variable through

$$u = \frac{1}{2} - \cos 2\theta \qquad \ldots (3.11)$$

gives an expression for v from equation 3.9 (b) as

$$v = \frac{1}{2} + \cos\left(2\theta - \pi/3\right) \qquad \ldots (3.12)$$

Substituting equation 3.11 in equation 3.6 (a) and with a change of independent variable from t to $\xi = e^t$ we get :

$$\frac{d\xi}{\xi} = \frac{2\sin\left(2\phi + \pi/3\right)}{1/4 - \cos^2 2\phi}\, d\phi \qquad \ldots (3.13)$$

where $2\phi = 2\theta - \pi/3$

Hence

$$\frac{d\xi}{\xi} = \frac{1/2\; d(\cos 2\phi)}{\cos^2 2\phi - 1/4} + \frac{\sqrt{3}\cdot 1/3\; d(\sin 2\phi)}{\sin^2 2\phi - 3/4} .$$

giving (by choosing a proper starting point for time)

$$\tan\phi - \pi/6 = \xi$$

$$\Rightarrow \tan\phi = \frac{\xi + 1/\sqrt{3}}{1 - \xi/\sqrt{3}} . \qquad \ldots (3.14)$$

Substituting this back in equation 3.9(b) we get

$$u = \frac{1 + \xi\sqrt{\xi}}{1 + \xi^2} \qquad \cdots (a)$$

$$v = \frac{1 - \xi\sqrt{\xi}}{1 + \xi^2} \qquad \cdots (b) \qquad (3.15)$$

Now in case we choose the negative sign in equation 3.9(b) the two curves get interchanged.

Although the represented coupled differential equation is a better approximation to the Central Difference Scheme, it is not adequate when the R.H.S. of equation 3.6 vanishes. So we have to introduce the h^3 term also. Then the equations are

$$\frac{2h^3}{6}\frac{d^3u}{dt^3} + 2h\frac{du}{dt} = 2h\,v(1-v) \qquad \cdots (a)$$

$$\frac{2h^3}{6}\frac{d^3v}{dt^3} + 2h\frac{dv}{dt} = 2h\,u(1-u) \qquad \cdots (b) \qquad (3.16)$$

In equation 3.16, the third derivative term starts an odd-even asymmetry very near u,v $\sim$1.0. This asymmetry is not due to the least count of the machine but due to the h^3-term. Due to this asymmetry one of u or v will be appreciably away from unity when the other is near 1.0 . Let,

$$\Delta = u - v .$$

$$\phi = \frac{u+v}{2} .$$

Then equation 3.16 becomes

$$\frac{d\Delta}{dt} + \frac{h^2}{6}\frac{d^3\Delta}{dt^3} = \Delta(2\phi - 1) \qquad \cdots (a)$$

$$\frac{d\phi}{dt} + \frac{h^2}{6}\frac{d^3\phi}{dt^3} = \phi(1-\phi) + \frac{1}{4}\phi\Delta^2 \cdots (b) \qquad (3.17)$$

If h is small, the equations and hence the solution would be similar to those of equation 3.6 as Δ is 'small' in some sense. A quick estimate of Δ can be obtained if in equation 3.17(a) we substitute equation 3.2 for ϕ. Since we are interested in the values of u,v, $\phi \sim 1.0$, the R.H.S. of equation 3.17(a) can be approximated by Δ itself. Hence we have

$$\Delta = \Delta_0 e^t$$

Thus the value of Δ increases exponentially. This explains the onset of zig-zag in the curve before the actual chaos starts. This exponential growth of zig-zag is illustrated in Fig 3.4 and Fig 3.5 for the step sizes of h=0.1 and h=0.01 respectively.

3.5 : Mixed Difference Scheme and Connection with Hénon Heiles Oscillator.

Yamaguti and Ushiki used a mixture of Euler's finite difference scheme together with the Central Difference Scheme to prevent the chaotic behaviour. Chaos can also be eliminated using the Predictor - Corrector method. They considered the mixed difference scheme parametrized by μ, $0 < \mu < 1$ for the ordinary differential equation 3.1. Equation 3.1 can be written in the form

$$(1-\mu)\frac{u_{n+1}-u_{n-1}}{2h} + \mu\frac{u_{n+1}-u_n}{h} = u_n(1-u_n) \quad \ldots(3.18)$$

Alternatively

$$u_{n+1} = \frac{1-\mu}{1+\mu} u_{n-1} + \frac{2}{1+\mu}\left[(\mu+h)u_n - h u_n^2\right]$$

which is the same as

$$u_{n+1} = \frac{1-\mu}{1+\mu} v_n + \frac{2}{1+\mu}\left[(\mu+h)u_n - h u_n^2\right]$$

$$v_{n+1} = u_n .$$

Then for sufficiently small time h with $\mu > h/2$, the solution of equation 3.18 is non-chaotic for $0 < t < \infty$. For a small h with $0 < \mu < h/2$, the solution after initially converging to a saddle point then repeats the cycles which were got earlier. These cycles then gradually deform and finally the solution converges to a sequence of period two. For $\mu \simeq h/2$, near 1.0, u_n converges to a periodic sink of period two. Thus for $\mu > h/2$ the fixed point (1,1) is a sink and for $\mu < h/2$ it becomes a hyperbolic fixed point.

Transforming the equation 3.18

$$u_n = \frac{\mu+h}{2h}\left[\left(\frac{h-\mu}{1+\mu}\right)x_n + 1\right]$$

$$v_n = \frac{\mu+h}{2h}\left[\left(\frac{h-\mu}{1-\mu}\right)y_n + 1\right]$$

into the form

$$x_{n+1} = y_n + 1 - a x_n^2$$

$$y_{n+1} = b x_n .$$

where

$$a = \frac{h^2 - \mu^2}{(1+\mu)^2}$$

and

$$b = \frac{1-\mu}{1+\mu}$$

we get the Hénon mapping which for certain particular value produces the Hénon-Heiles strange attractor.

CHAPTER - IV

STRANGE ATTRACTORS IN THE COMPOSITION OF TWO SIMPLE HARMONIC MOTIONS

4.1 : Introduction

In chapter II we had discussed the Hénon-Heiles attractor. Now we discuss a much simpler system which exhibits a similar chaotic approach which is invariant under scaling by the study of composition of two simple harmonic motions in mutually perpendicular directions :

$$x = \cos t$$
$$y = \cos(\beta t + \theta + \pi/2) \qquad \ldots (4.1)$$

for different values of β

4.2 : β is rational.

In equations 4.1, if $\theta = (2k+1)\pi/2$ then is represents a circle and if $\theta = (2k\pi)$, k an integer, we get a straight line. For all other values of θ we get an ellipse.

Now we consider a slightly different set of simple harmonic motions with $\beta = M/N$ where $M \approx N$ are large integers. Also

$$x = \cos t$$
$$y = \cos((M/N)t + \theta + \pi/2) \qquad \ldots (4.2)$$

For a small enough range of time $t \approx 2\pi$ since $M \approx N$, the motion represented by equation 4.2 is quite similar to that of equation 4.1, i.e., it would appear almost like a closed elliptic orbit. However, after each loop around the orbit, due to the difference of M/N from 1.0, the effective value of θ would change by $(M/N).2\pi$ approximately. Consequently the shape of the ellipse changes continuously. From a shape at sometime almost close to the straight line $y = x$, through an elliptic orbit it changes to a circular orbit and then to a shape close to the straight line $y = -x$, then through a circular orbit back to the original line. Thus one expects the value of the distance of the point from the origin given by

$$R = (x^2 + y^2)^{1/2} \qquad \ldots(43)$$

to oscillate with a period of approximately π, the successive minima (maxima) starting near 1.0 and monotonically decreasing (increasing) at the beginning. This process continues till θ (in the equation 4.2) reaches $\pi/2$. Then onwards the minima (maxima) start increasing (decreasing) monotonically. The complete trajectory has a period $N\pi$.

Three cases of interest are discussed below.

When N is even (and M = N + 1), the minimum

value of R is of the order of 1/N and the maximum value is exactly $\sqrt{2}$. In this case after N/2 loops about the origin the value of R reaches its maximum value, and the curve retraces its path. The trajectory of one particular case of this type with N = 10 and M = 11 is shown in Fig. 4.1.

On the other hand if M is even and N = M + 1, the minimum value of R is exactly zero but the maximum value of R is not exactly $\sqrt{2}$. In fact we have

$$\sqrt{2} - R_{max.} \sim O(1/N^2) \qquad \ldots(4.4)$$

This case is illustrated in Fig. 4.2 for M =10 and N = 11.

If M,N are both odd, the trajectory will neither reach the origin nor $\sqrt{2}$, through it goes near these points at distances comparable to the above cases.

4.3 : β is irrational.

We now consider a generalisation of the equation where M/N is replaced by an irrational number. Then we have after scaling the time by a factor of β in equation 4.2

$$x = \sin t$$
$$y = \cos \beta t \qquad (4.5)$$

Since every irrational number β can be approximated by a rational number of the form M/N (M,N having no common

factorδ, the orbit will have the features of the above types of trajectories.

For times smaller than $N\pi$, the smallest of the minima is of the order of 1/N. Then the largest of the maxima is of the order of $\sqrt{2} - O(1/N^2)$. A better rational approximation to β, M_K/N_k (where at a time of the order of $1/N_k$. In between these two times the minimum value of R decreases at first as with each loop the phase difference between the two simple harmonic motions gets built up till it reaches and then onwards the minimum value of R starts increasing.

Now in order to study the chaotic behaviour near strange attractors in the Hénon-Heiles oscillator we choose a specific value of β which shows infinite number of such close approaches to the origin, eabh succossive denominator increasing approximately by a factor of ten. The β we chose is

$$\beta = 1 + \varepsilon = 1 + \cfrac{1}{10 + \cfrac{1}{10 + \cfrac{1}{10 + \cdots}}} \qquad \ldots (4.6)$$

$$= \sqrt{26} - 4 \simeq 1.0990198\ldots$$

The partial convergents to (see appendix)

$$\frac{M_K}{N_K} = \frac{11}{10}, \frac{111}{101}, \frac{1121}{1020}, \frac{11321}{10301}, \ldots\ldots (4.7)$$

are the best approximations to β in the following sense : For every positive integer $N < N_k$ and for all integers M,

$$\left| \frac{M}{N} - \beta \right| > \left| \frac{M_k}{N_k} - \beta \right| \qquad \ldots(4.8)$$

So we expect (in time scales of the order of $N_k \pi$), to find the value of R to approach 0.0 (or $\sqrt{2}$) to an approximation of the order of $1/N_k$ (or $1/N_k^2$). On a machine with 10 digit accuracy it is difficult to demonstrate the behaviour near the maxima. For, even with k = 4, $1/N_k^2$ falls below the least count of the machine and hence only k = 2 can be studied.

In the following we study the approach of R to zero in four different generations.

From the discussion following equation 4.5, in view of equation 4.8 it is clear that the closest approach occurs only at times approximately $(N_k/2)$ when N_k is even (times corresponding to $N_k \pi$, with N_k odd will lead to maxima closer to $\sqrt{2}$).

To start with we describe the behaviour in detail for the time $0 < t < 10\pi$. During this period 11/10 is a good approximation to β . The dependence of R on t for this range is shown in Fig. 4.3.

The value of R in equation 4.5, initially, at t = 0 is 1.0. But as time increases the phase difference

between x and y increases from $\pi/2$ and so the value of R decreases first. A better representation of R is given by

$$R = \left[1 - \sin\{(2+\varepsilon)t\} \sin(\varepsilon t) \right]^{1/2} \qquad \ldots (4.9)$$

where $\varepsilon = \beta - 1 \approx 0.0990198 \ldots$

From equation 4.9 it appears that the first minimum with a value of R = 0.96 occurs when 2t exceeds $\pi/2$ slightly, for at this value of t, $\sin\{(2+\varepsilon)t\}$ reaches its maximum value and $\sin(\varepsilon t)[<0.1]$ changes slowly. As t continues to increase, the value of R increases till it reaches its next maximum value when $2t \simeq 3\pi/2$. Then onwards the minima (maxima) keep decreasing (increasing) monotonically till $2\varepsilon t \approx \pi, (t \simeq 5\pi)$. At $t \simeq 5\pi$, the minimum value of R = 0.025. The nearby maximum value of R is approximately $\sqrt{2}$. Now, as t increases the minima (maxima) of R start increasing (decreasing) monotonically till around $t = 10\pi$, then onwards the same behaviour described above gets repeated for some more cycles. This pattern resembles the amplitude modulated radio frequency signal.

From equation 4.9, since $\varepsilon \approx 1/10$ we expect a R_1 (the minimum value of R in each loop of 10 cycles each of time period π) to be smaller than 0.1. In this range there is only one value of t where $R_1 < 0.1$. A local minimum (<0.2) can occur only when $\beta t \approx (n + 1/2)\pi$,

where n is a positive integer. As $\varepsilon \approx 0.1$, this can happen approximately at intervals of 10π. Now we study the local minima of R (within each loop of 10π, R_1), in the region $0 < t < 1020\pi$. The first R_1 occurs around $t = 5\pi$, as was discussed earlier. (See Fig 4.4)

For $t = n\pi$, let $\beta t = (m + 1/2)\pi + \delta$ and δ_n be $[Fr\{(\beta t)/\pi - 1/2\}]\pi$. For $t = 5\pi$ we get $\delta = -0.1540144\ldots$ Also,

$$R_{(min)_n} \simeq \frac{\delta_n}{2}$$

For every increase in t by 10π the δ_n increases by -0.031. (see table 4.1). So after $|\delta_n|$ exceeds a value $\Delta/2$ where

$$|\Delta| = |Fr(\beta)\pi| > 0$$

i.e. $\Delta \simeq 0.1$.

it is more advantageous to add a π to the value of t ($t \simeq 55\pi$) to find a local minimum than to add another 10π. Addition of π changes the sign of the phase difference (- to +) to approximately $\Delta/2$. Then onwards for the next ten loops the phase difference keeps decreasing by 0.031 (see table 4.1). Consequently R_1 also starts decreasing per each loop and near $t = 106\pi$. The value of R_1 ($\simeq 0.008$) is lower than the previous value (near $t = 5\pi$). The value of R at this time (R_s) is the lowest in a super loop of 101π (from 56π to 157π) We continue this till the value of $|\delta|$ just exceeds $\Delta/2$, when we add a π to t to get the next minimum. This process is repeated for each super loop

of 101π (10 loops + 1 cycle). The local minima, R_s, in each super loop near $t \simeq 5\pi$, 106π, 207π , 308π, etc. are successively smaller than the previous ones till $t=510\pi$ The global minimum of the grand loop $0<t<1020\pi$ is attained at $t = 510\pi$. Till $t = 510\pi$

$$R_{s+1} - R_s < 0$$

But for $t > 510\pi$ we get

$$R_{s+1} - R_s > 0$$

The value of R_s near $t = 510\pi$ is approximately 1/100 of the value of R at $t = 5\pi$. Smimlarly the minimum value R_s in the next grand loop $1020\pi < t < 2040\pi$ occurs near $t = 1530\pi$ and has a value 1/100 that of R at $t = 15\pi$. This process is repeated in the next two generations which are illustrated in Fig. 4.5 and Fig. 4.6. This process keeps repeating ad infinitum when the time scale is magnified by a hundred each time.

CHAPTER - V

CONCLUSION

In this dissertation we have just briefly studied the concept of strange attractors and the behaviour of the trajectories near them. We supported this concept by a few examples.

In the beginning a brief introduction to ordered dynamical systems was given. Then the concept of strange attractors was introduced. In Chapter II we saw a few examples of this in different models. This was followed by the study in detail of the chaos in central difference scheme for logistic equations. An analytical explanation of the occurrence of chaos was also given.

An original contribution of this dissertation is the phenomenon of self-similarity under scale-invariance near strange attractors in the composition of two simple harmonic motions in mutually perpendicular directions.

In recent times there has been a lot of development in this topic. It has applications in a vast range of subjects. To name a few, we have evolution of species and Volterras equation (Scudo, F.M. and James R. Zeigler 1978); turbulence of fluids (Lorenz 1963;

Ruelle and Takens 1971) buckling beams (Holmes); Optics (Stewart 1981); blood production etc. Notable omissions in this dissertation are the work done by S. Smale, Volterra, Vander Pol, Ruelle and Takens, Lorenz and others. This topic has a lot of scope for further developments. Some of the properties of strange attractors such as dimension, correlation function, distribution function etc can be studied in more detail. S. Smale and Ushiki, S. have also done a lot of study of this concept with the help of dimension theory and topology.

APPENDIX

Here we list the results from the theory of continued fractions required in Chapter IV (Chrystal, 1964).

Any real number β can be expressed as a continued fraction:

$$\beta_n = a_1 + \cfrac{1}{a_2 + \cfrac{1}{a_3 + \cdots}} \qquad \ldots(A.1)$$

where a_1, a_2, a_3, . . . are positive integers. If β is rational, then this continued fraction is terminating ($a_n = 0$, n N).

The partial convergents to β are defined as

$$\beta_n = a_1 + \cfrac{1}{a_2 + \cfrac{1}{a_3 + \frac{1}{a_4} + \cdots + \frac{1}{a_n}}} = \frac{P_n}{Q_n} \qquad \ldots(A.2)$$

where P_n, Q_n are integers (mutually prime).

Then,

$$P_1 = a_1 \quad ; \quad Q_1 = 1$$
$$P_2 = a_1 a_2 + 1; \quad Q_2 = a_2 \qquad \ldots(A.3)$$

There is a recurrence relation between P's and Q's:

$$P_n = a_n P_{n-1} + P_{n-2}$$
$$Q_n = a_n Q_{n-1} + Q_{n-2} \qquad \ldots(A.4)$$

The fraction $\beta_n = P_n / Q_n$ is called the nth partial convergent. Then P_n, Q_n satisfy the following relations:

$$\frac{P_n}{Q_n} - \frac{P_{n-1}}{Q_{n-1}} = \frac{(-1)^n}{Q_n \cdot Q_{n-1}} \qquad \ldots (A.5)$$

$$\frac{P_n}{Q_n} - \frac{P_{n-2}}{Q_{n-2}} = \frac{(-1)^{n-1}\, a_n}{Q_n \cdot Q_{n-2}}$$

The odd convergents increase monotonically in value whereas the even convergents decrease monotonically. Every even convergent is greater than every odd convergent. Also these convergents P_n / Q_n tend to β as $n \to \infty$.

For all integers, P, Q such that $Q < Q_n$, :

$$\left| \beta - \frac{P_n}{Q_n} \right| < \left| \beta - \frac{P}{Q} \right|$$

If

$$\beta = 1 + \frac{1}{10 + \frac{1}{10 + \cdots}} = 1 + \frac{1}{9+\beta} = \sqrt{26} - 4 .$$

then the partial convergents are

$$1, \quad \frac{11}{10}, \frac{111}{101}, \frac{1121}{1020}, \frac{11321}{10301}, \frac{114331}{104030}, \frac{1154631}{1050601},$$

$$\frac{11660641}{10610040}, \ldots$$

For the problem in chapter IV, if the trajectory has to approach the origin then t/π, ($\beta t/\pi - 1/2$) have to be very close to integers and consequently this is expected to occur when

$$\frac{t}{\pi} = \frac{\pi}{2} \quad (Q_{2n})$$

TABLE 2.1

$\lvert x \rvert$	$\lvert \lambda_L \rvert$	$\lvert \lambda_s \rvert$
0.0	0.548	0.548
0.25	1.000	0.300
0.5	1.588	0.189
0.6315	1.924	0.156
0.75	2.134	0.134
1.00	2.903	0.103
1.25	3.583	0.083
1.50	4.270	0.070

NOTE : If $x > 0$, $\lambda_L < 0$, $\lambda_s > 0$ and vice-versa if $x < 0$.

The eigenvalue of the matrix $\begin{pmatrix} -2.8x & 1 \\ 0.3 & 0 \end{pmatrix}$

for different values of x.

TABLE 4.1

$t=n\pi$	δ_n	
8π	−0.01540	
15π	−0.04620	
28π	−0.07701	
35π	−0.10781	
48π	−0.13861	
55π	−0.16942	
$56\pi(65\pi)$	+0.14166	(−0.20042)
66π	+0.11086	
76π	+0.08006	
86π	+0.04925	
96π	+0.01845	
106π	−0.01236	

The phase difference between x and y at different instants of time. Note particularly at time $t=55\pi$ it is more advantageous to give a further step of π rather than 10π.

FIGURE CAPTIONS

		Fig. No.
1.	Nature of Critical Points : Node ($\lambda_1 < \lambda_2 < 0$)	1.1(a)
	Saddle ($\lambda_1 < 0 < \lambda_2$)	1.1(b)
	Nodes ($\lambda_1 = \lambda_2 \neq 0$)	1.1(c)
		1.1(d)
2.	Nature of Critical Points : Spiral (Re $\lambda < 0$)	1.2(a)
	Center (Re $\lambda = 0$)	1.2(b)
3.	The behaviour of the line segment A_1B_1 near an attractor —	2.1
4.	The normal and chaotic behaviour of the central difference scheme for logistic equation. —	3.1
5.	The behaviour of u and v near the origin for 6-digit accuracy —	3.2
6.	The behaviour of u and v near the origin for 5-digit accuracy —	3.3
7.	The exponential growth of zig-zag for step size h = 0.1 —	3.4
8.	The exponential growth of zig-zag for step size h = 0.01 —	3.5
9.	The motion of the trajectory for N = 10, M = 11 in equation 4.2 —	4.1
10.	The motion of the trajectory for N = 11, M = 11 in equation 4.2 —	4.2

***

FIG 1'1

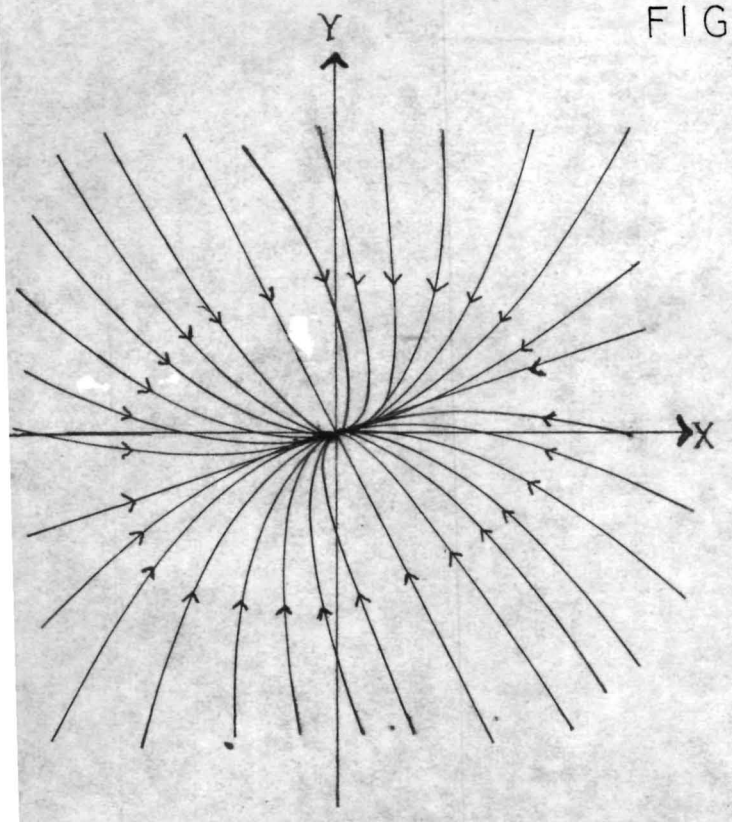

(a)

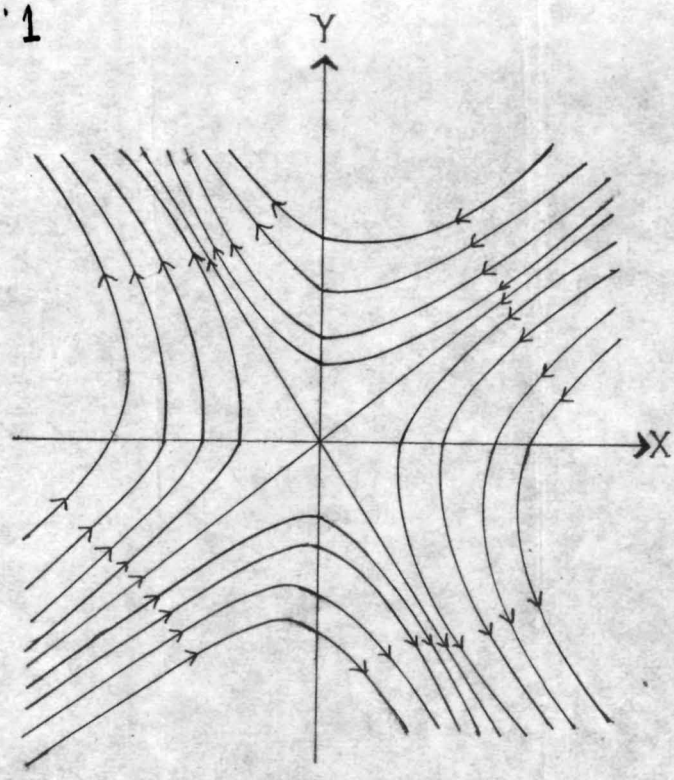

(b)

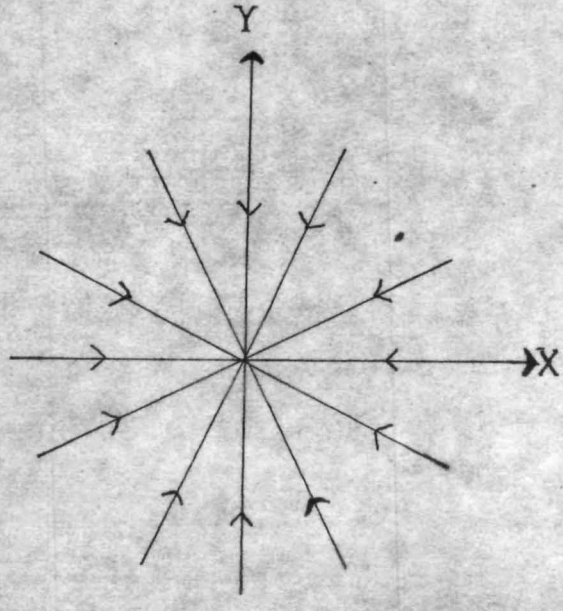

(c)

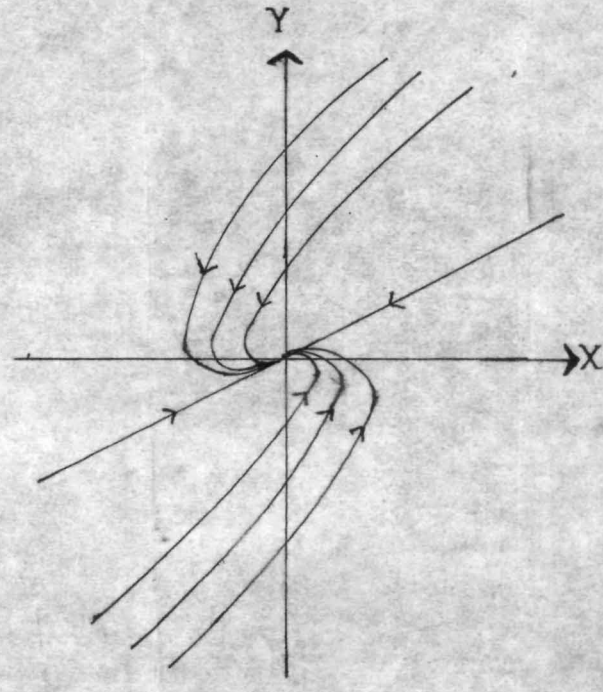

(d)

FIG 1·2

(1·2)

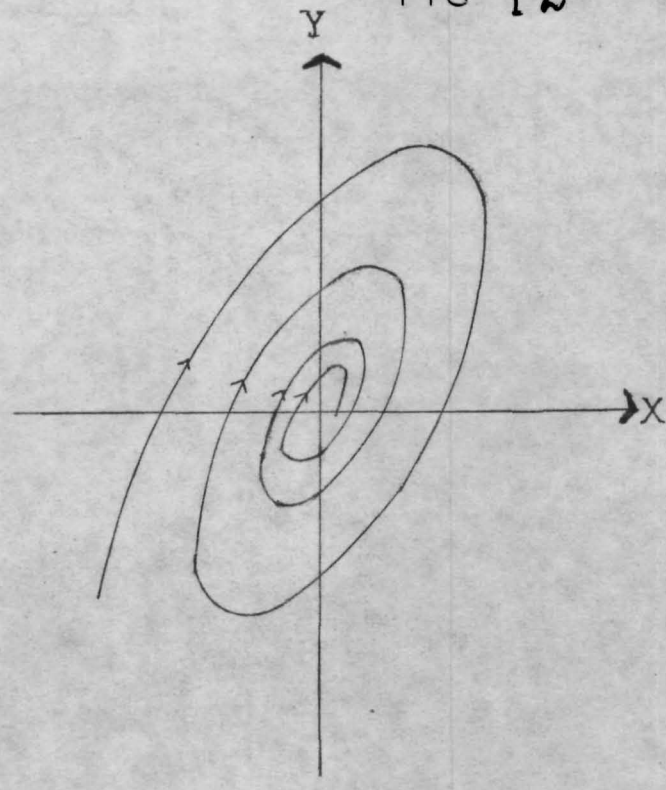

(a)

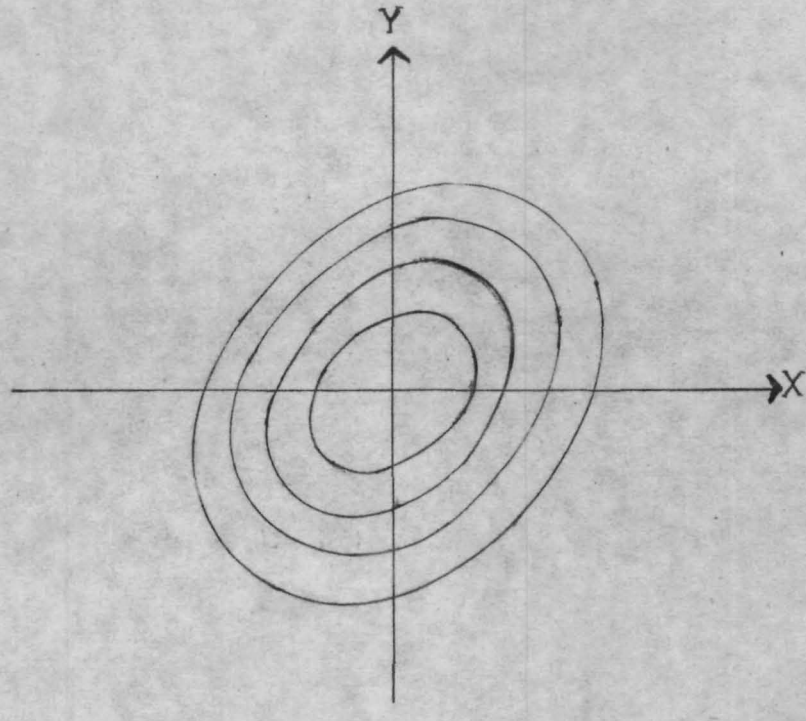

(b)

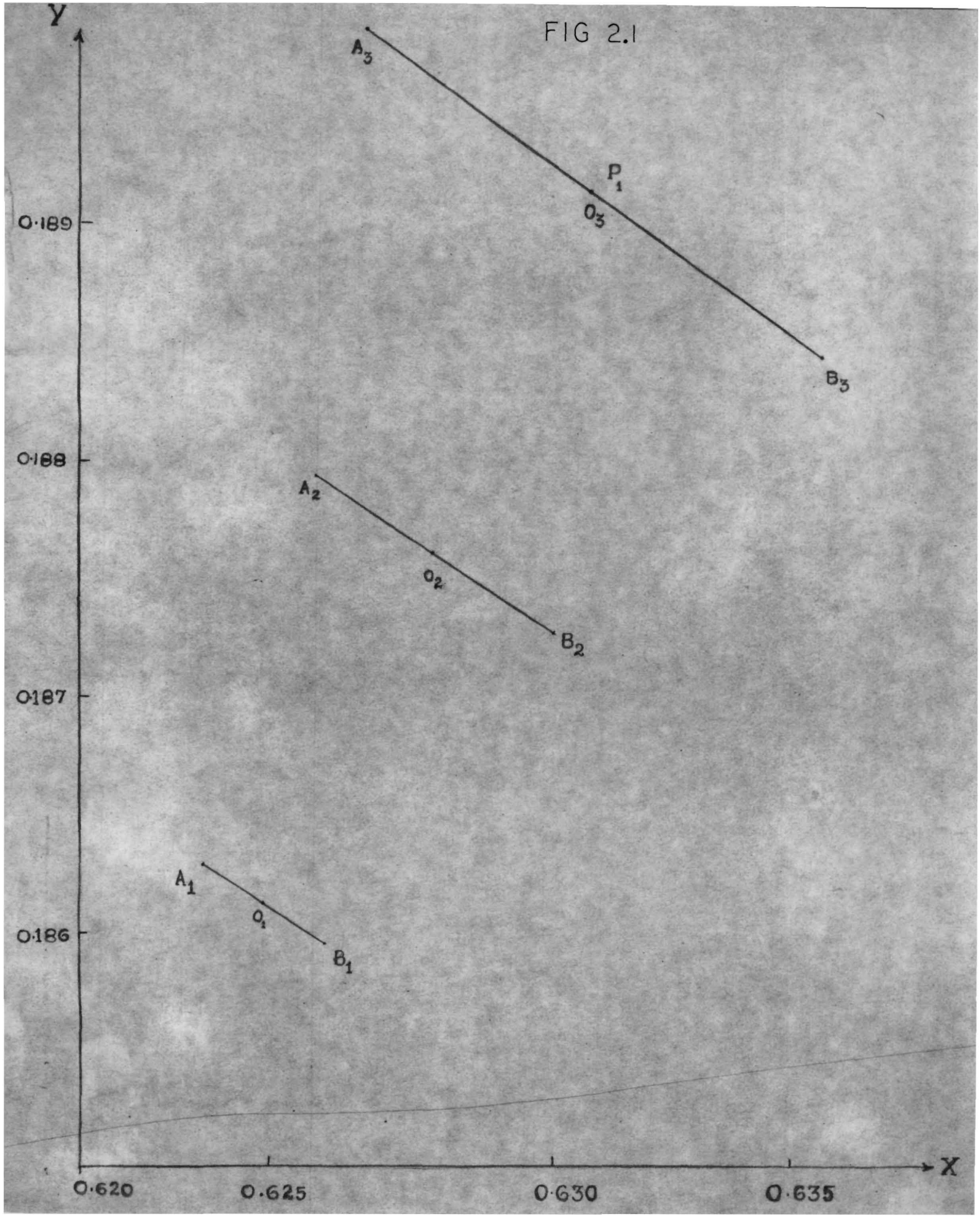
FIG 2.1
Y
X
A3
P1
O3
B3
A2
O2
B2
A1
O1
B1
0·189
0·188
0·187
0·186
0·620
0·625
0·630
0·635

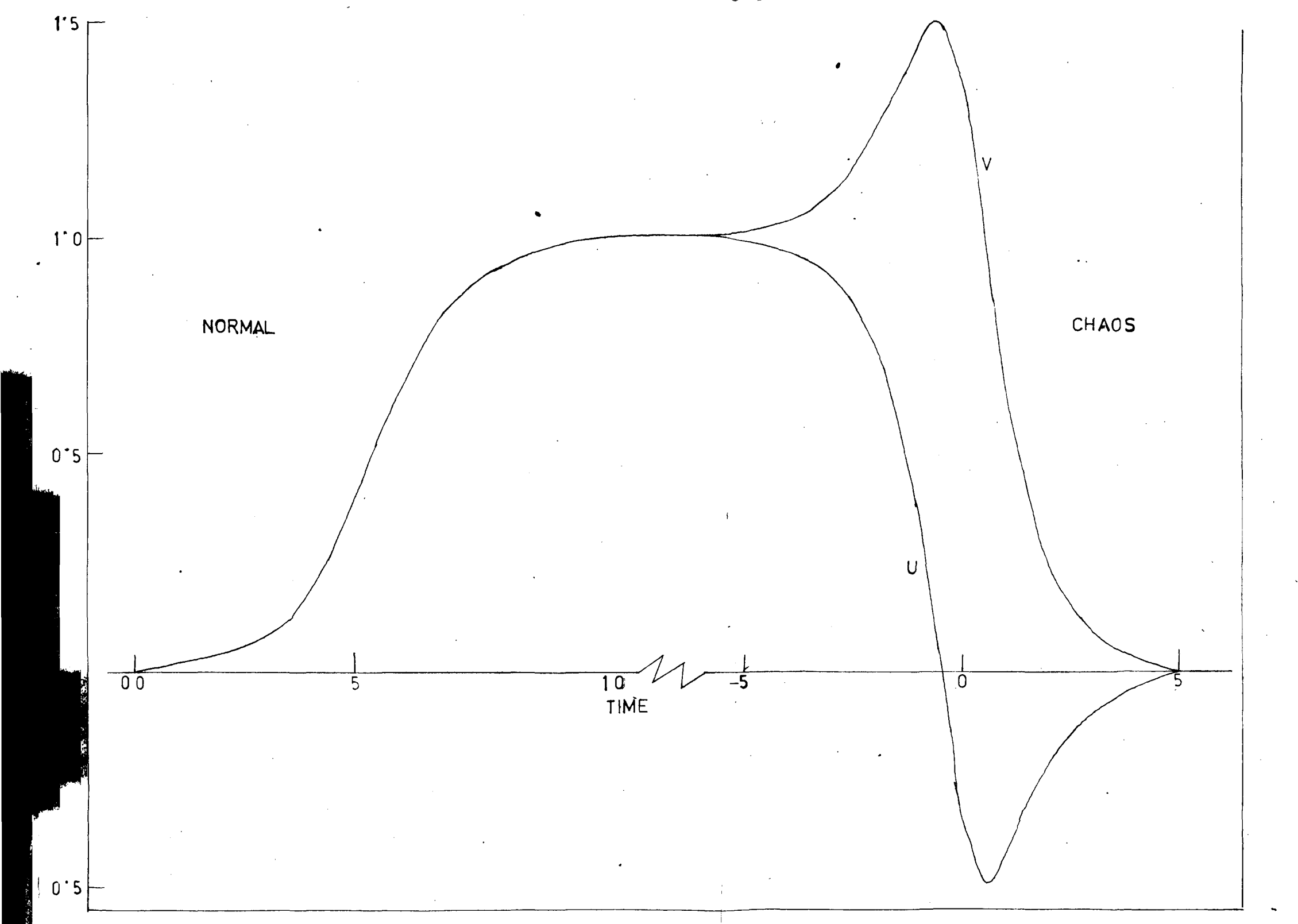
1·5
1·0
0·5
0·5
NORMAL
CHAOS
V
U
00
5
10
-5
0
5
TIME

FIG 3·2

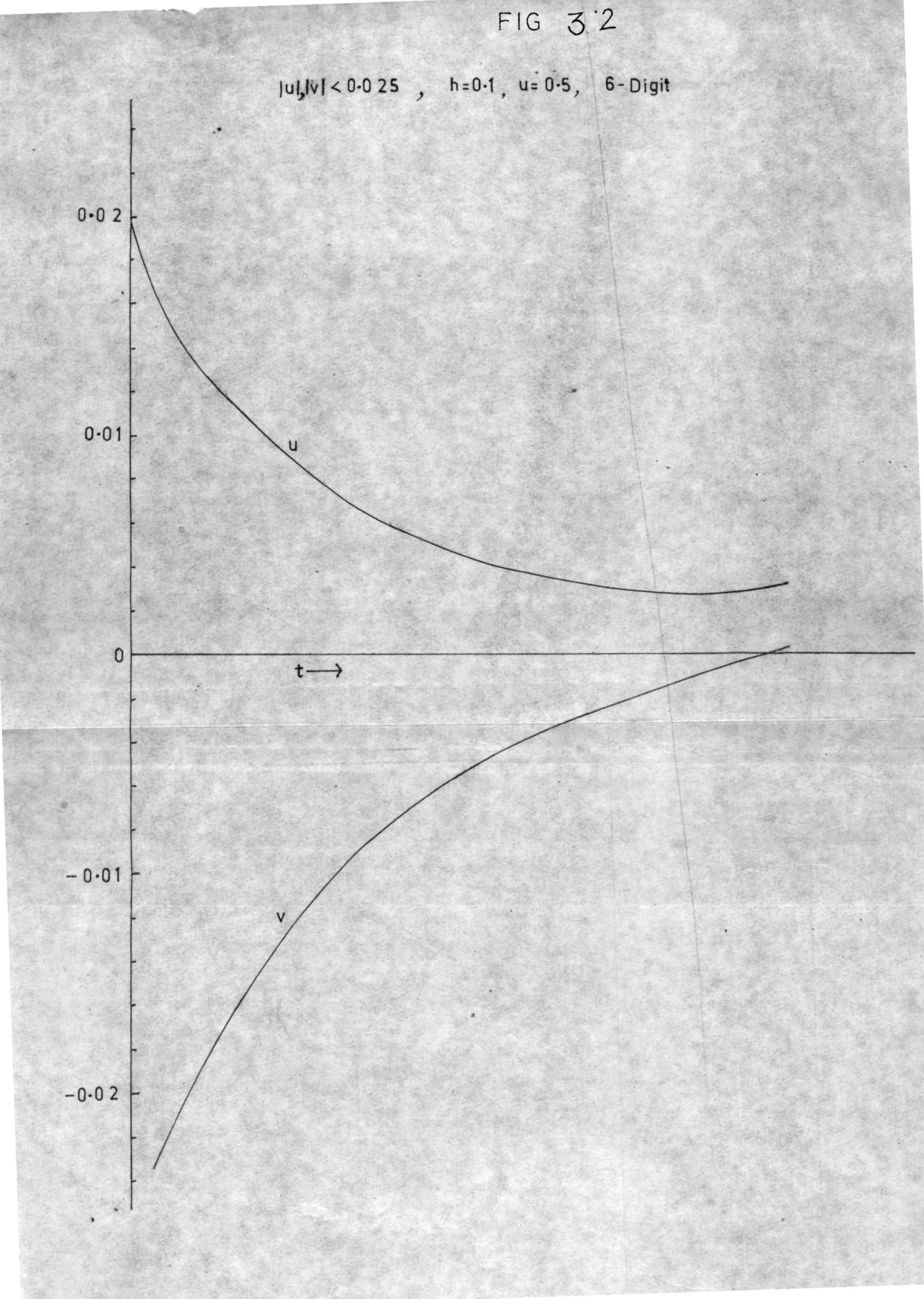

FIG 3.3

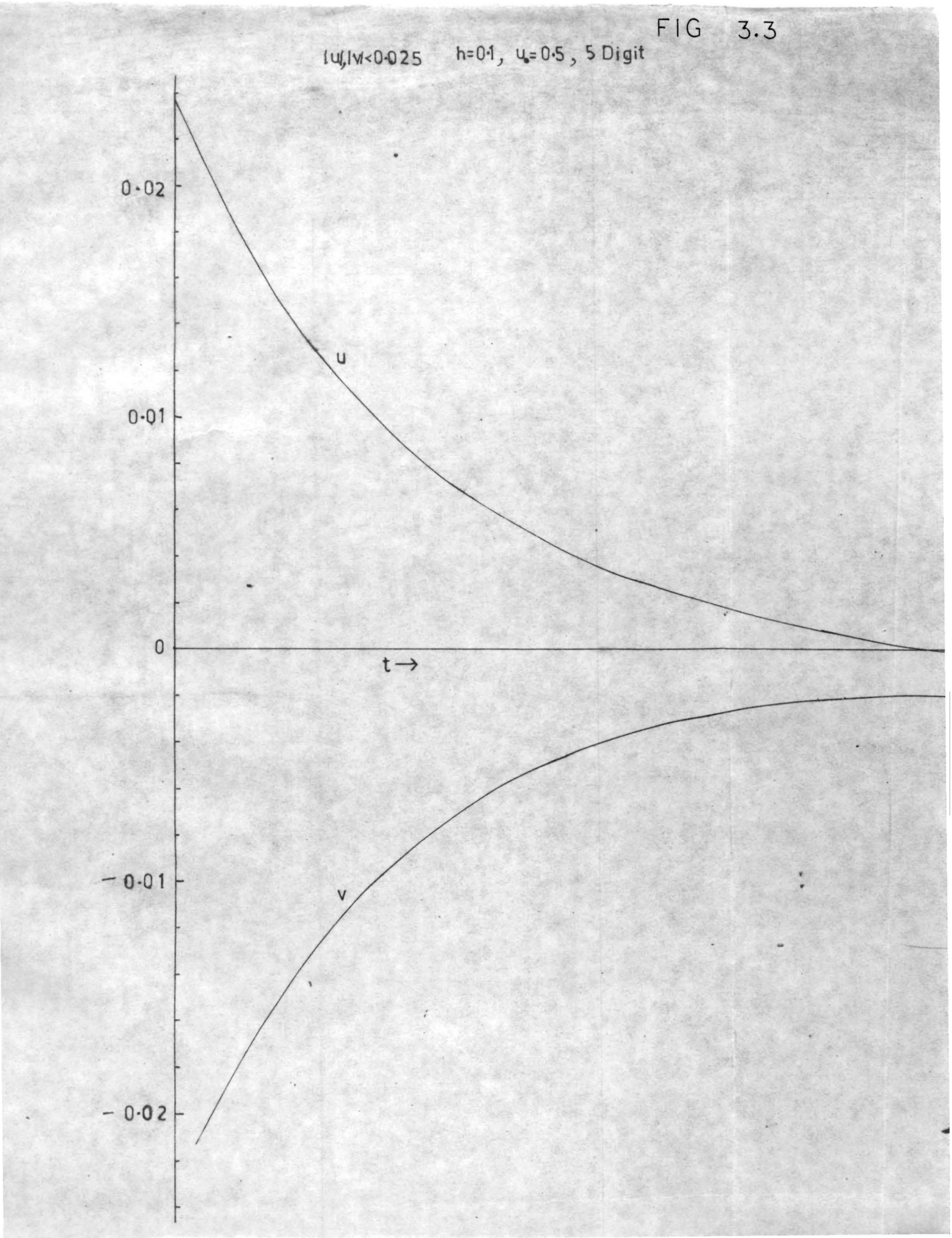

FIG 3.4

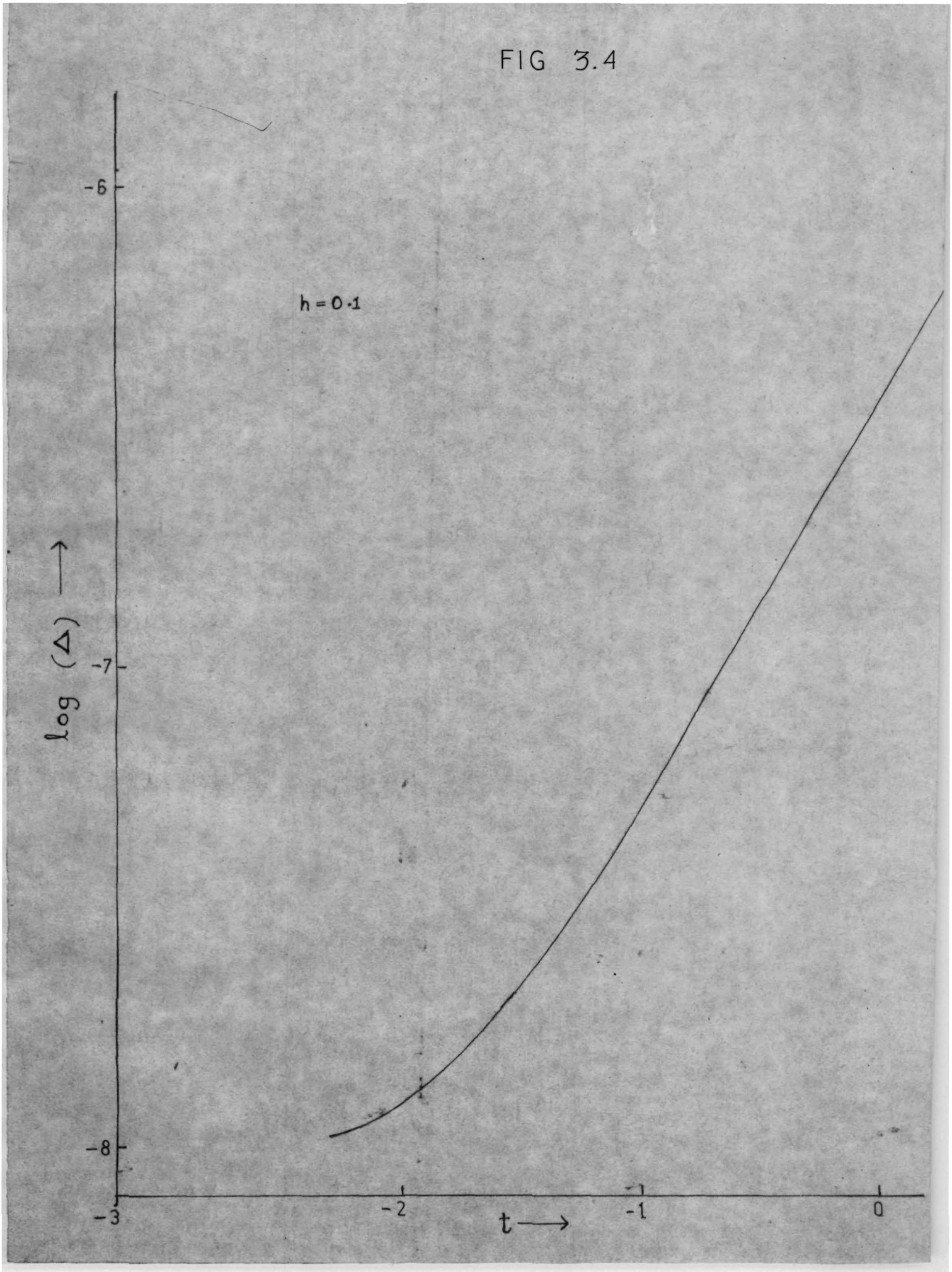

FIG 3.5

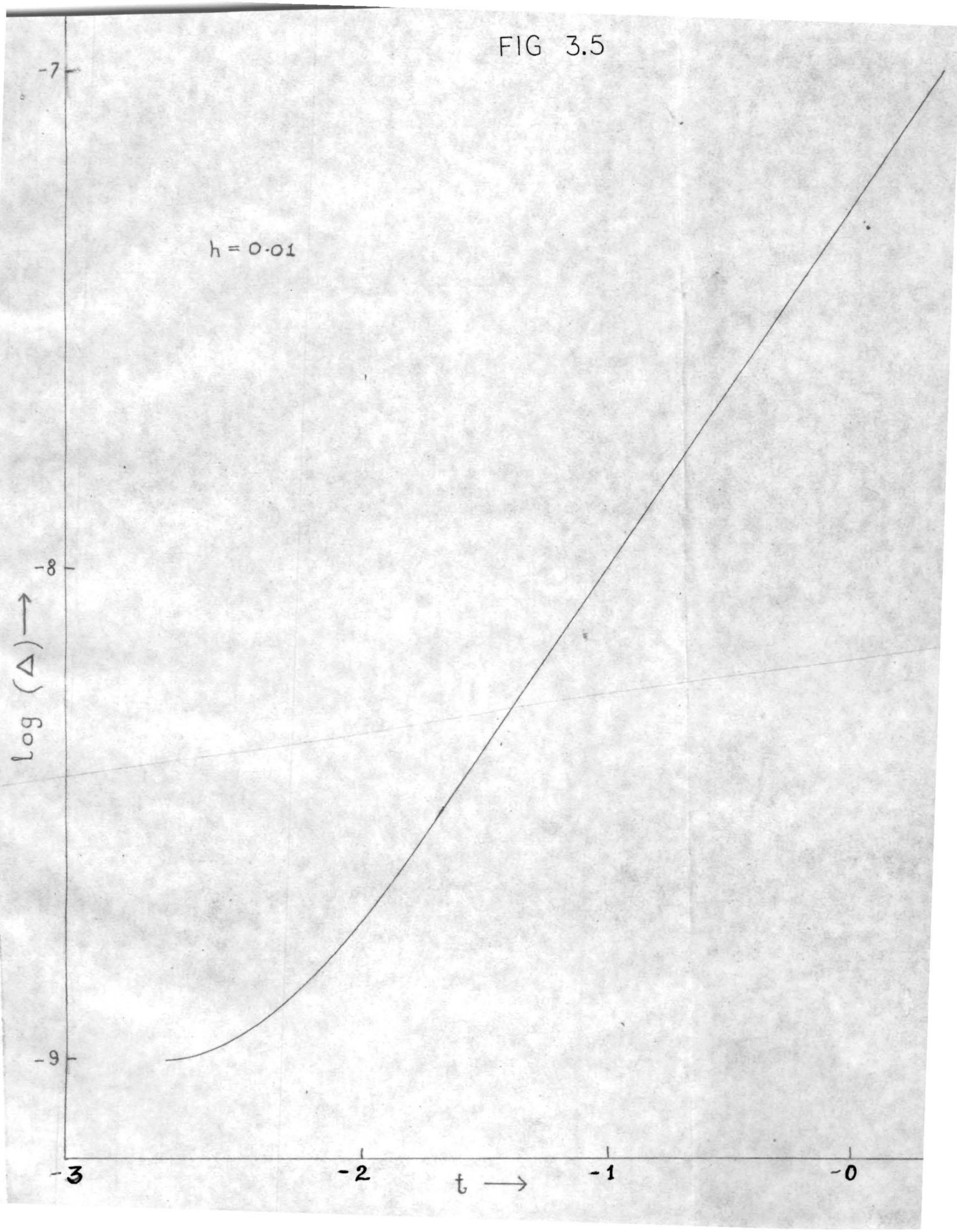

FIG 4·1

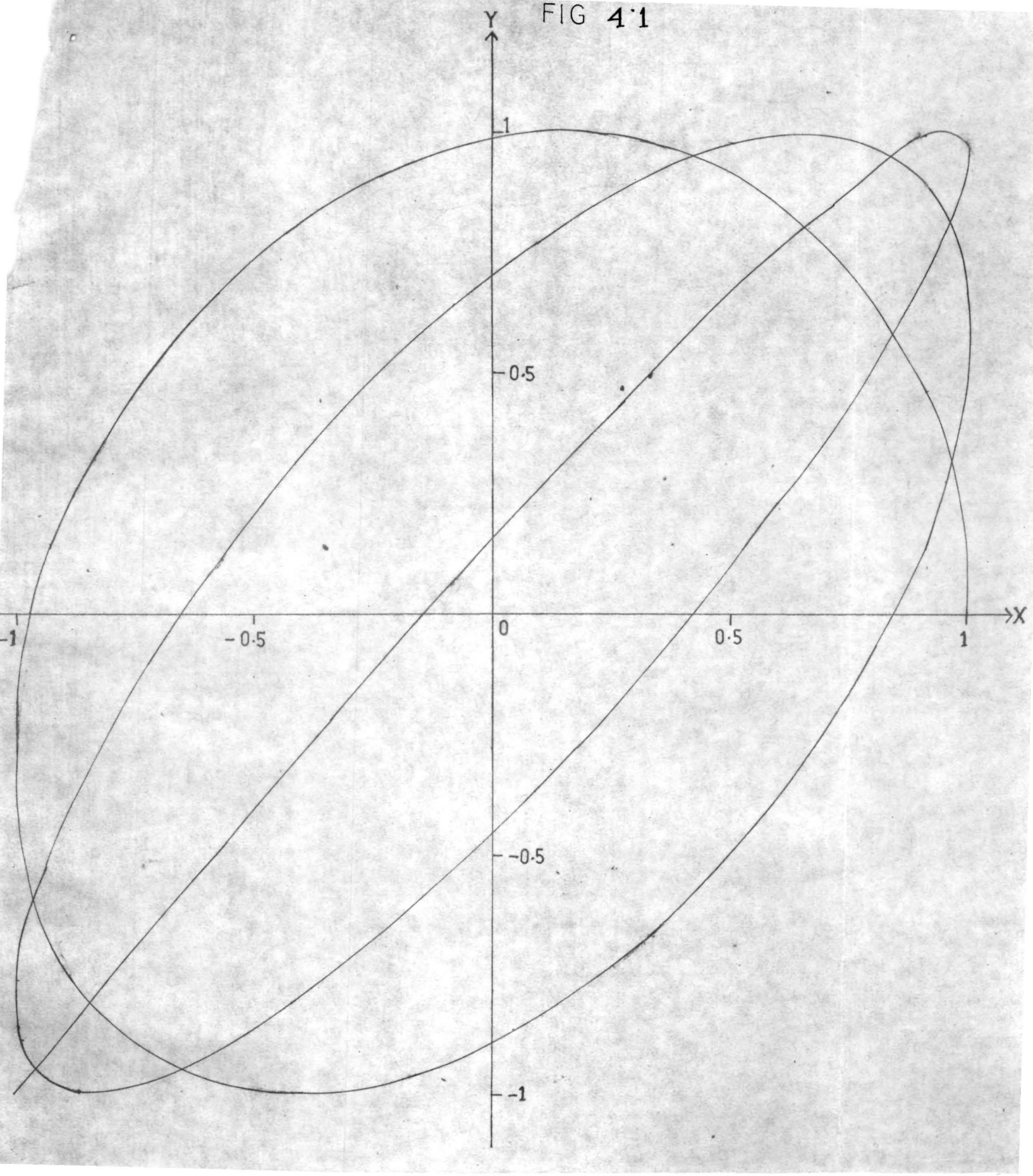

FIG 4.2

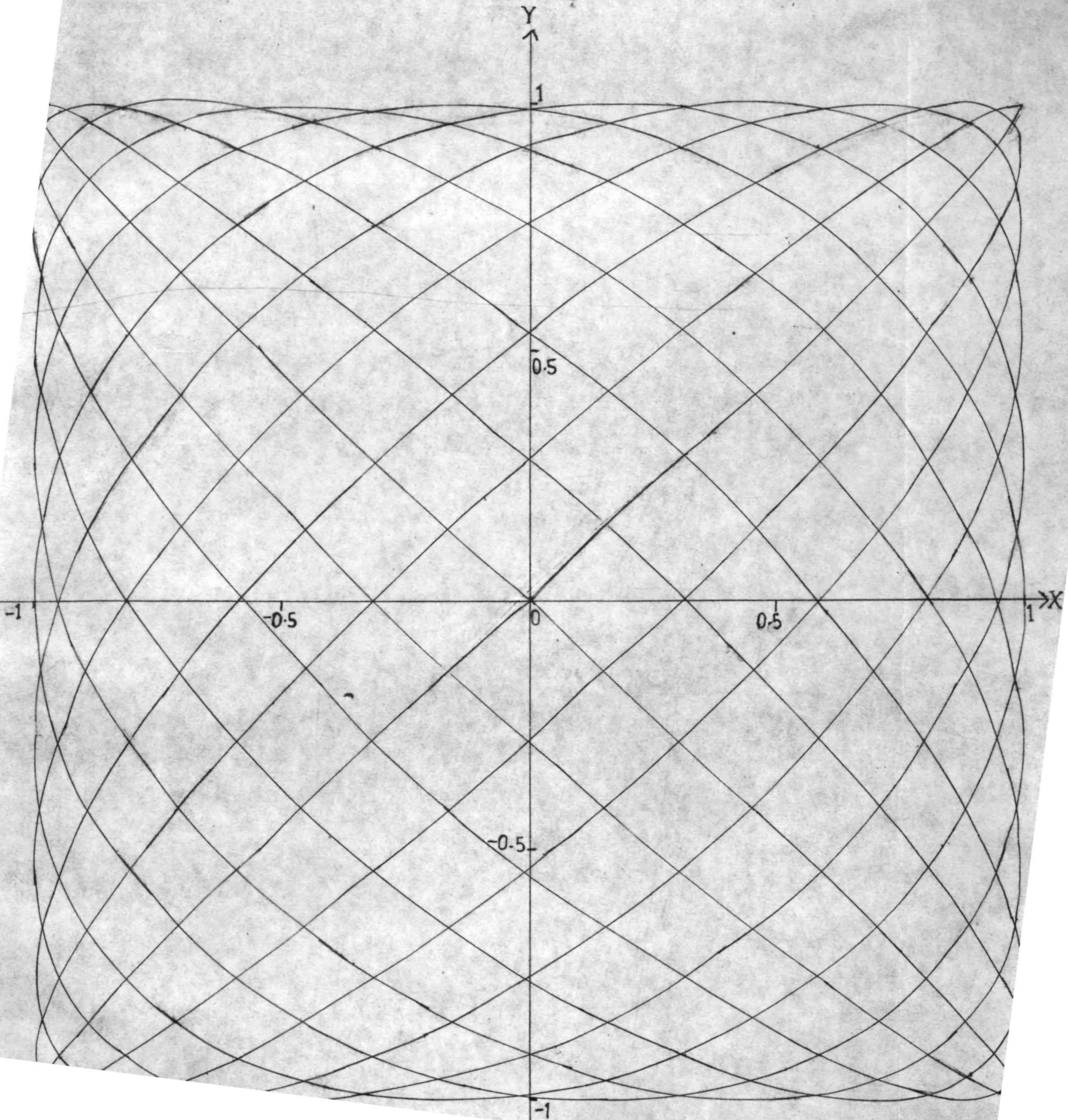

FIG 4·3

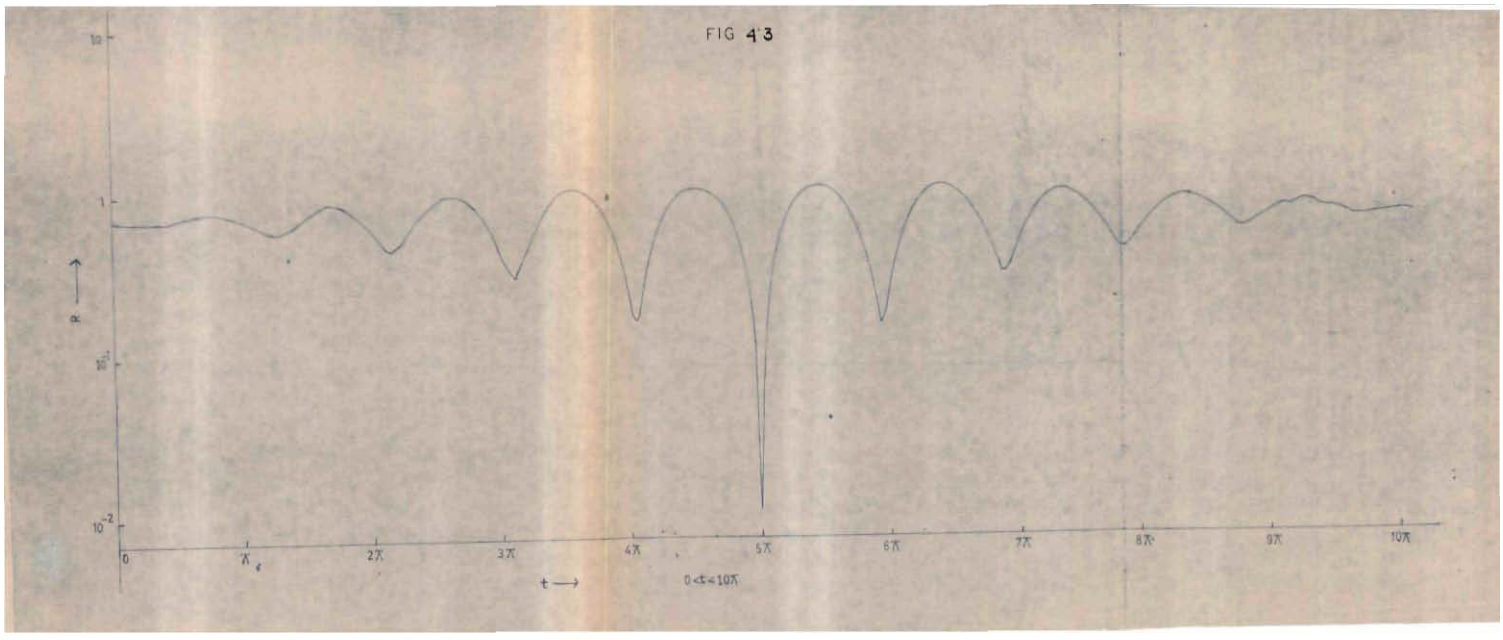

FIG 4.4

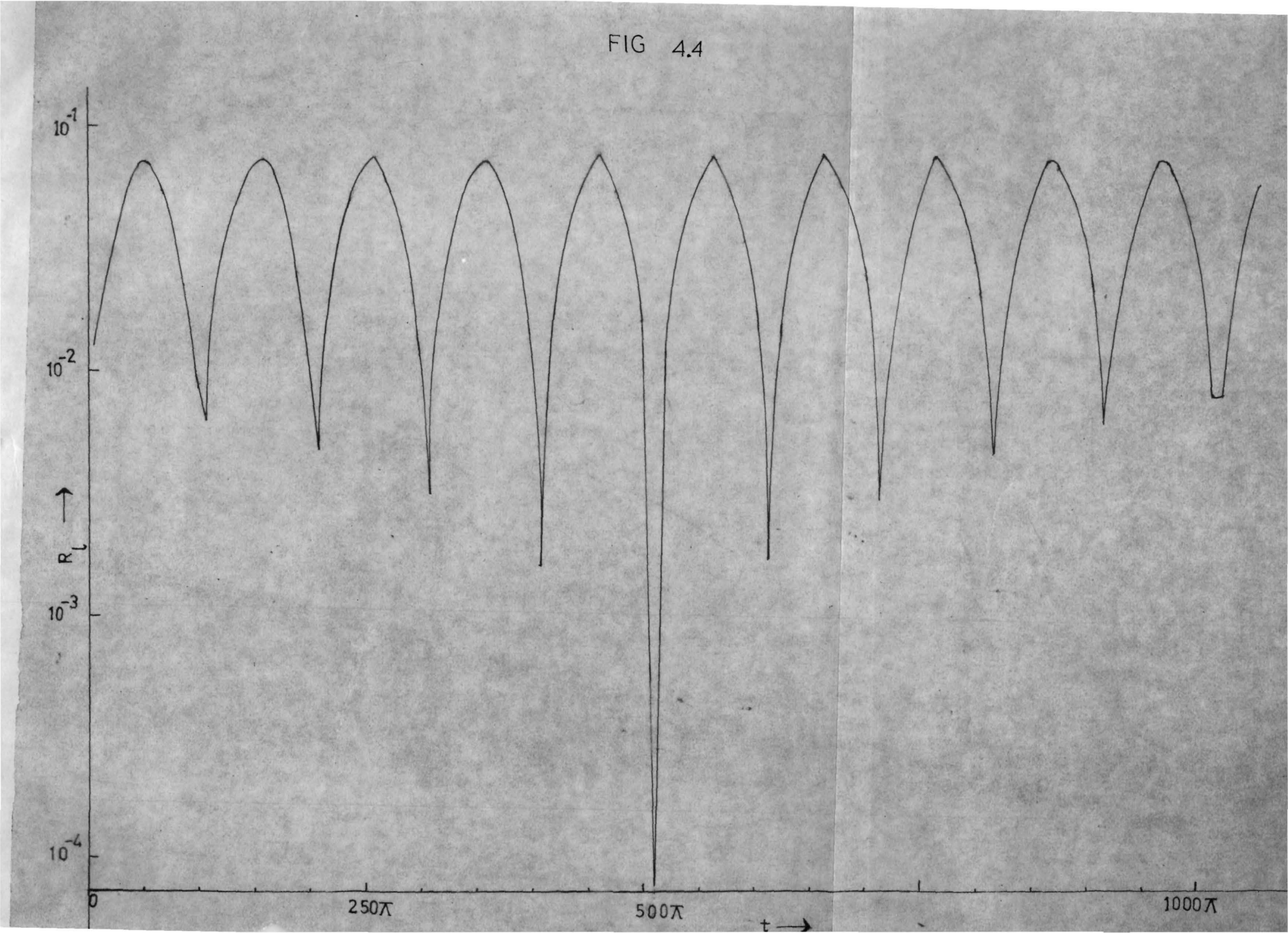

FIG 4·5

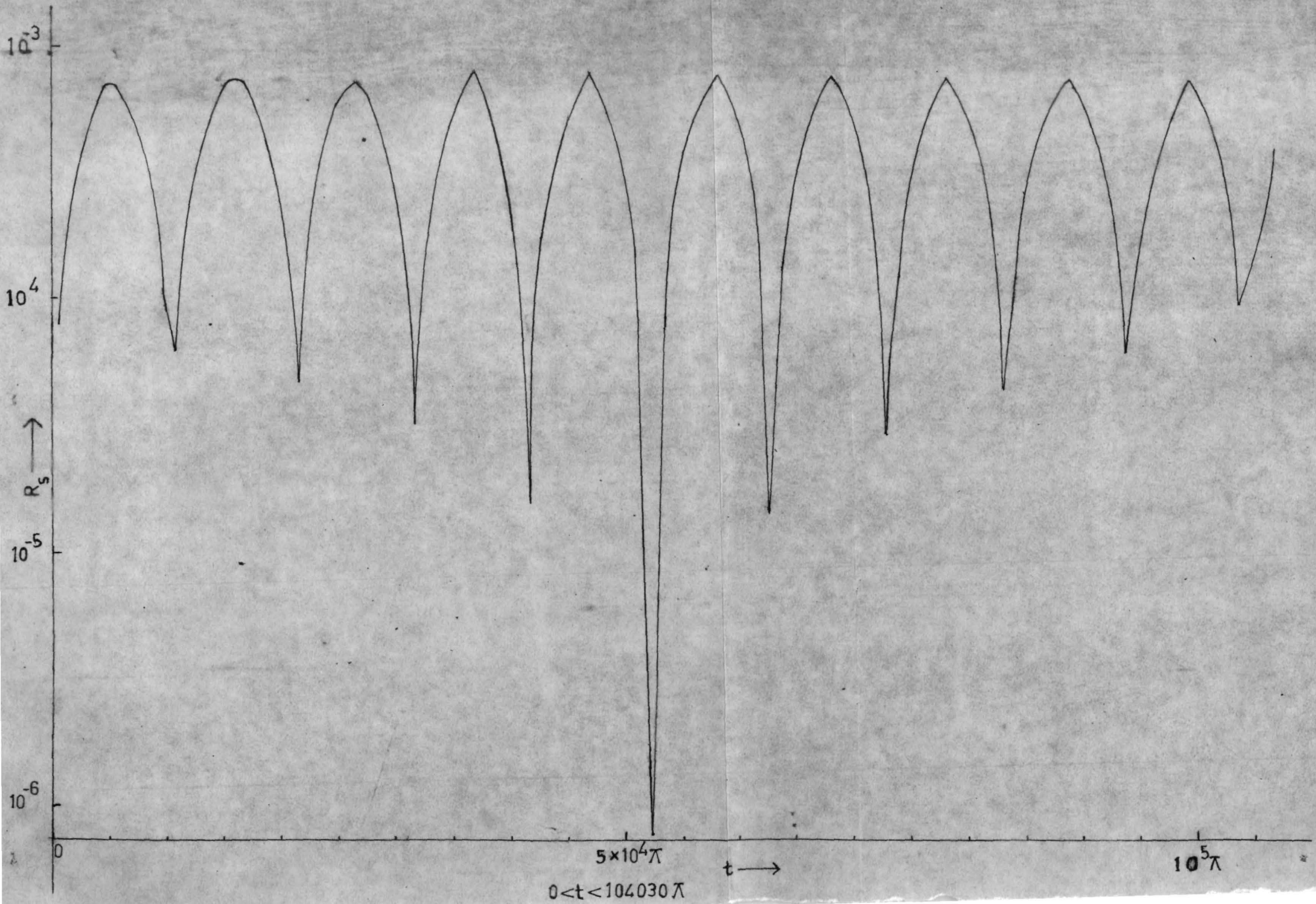

FIG 4·6

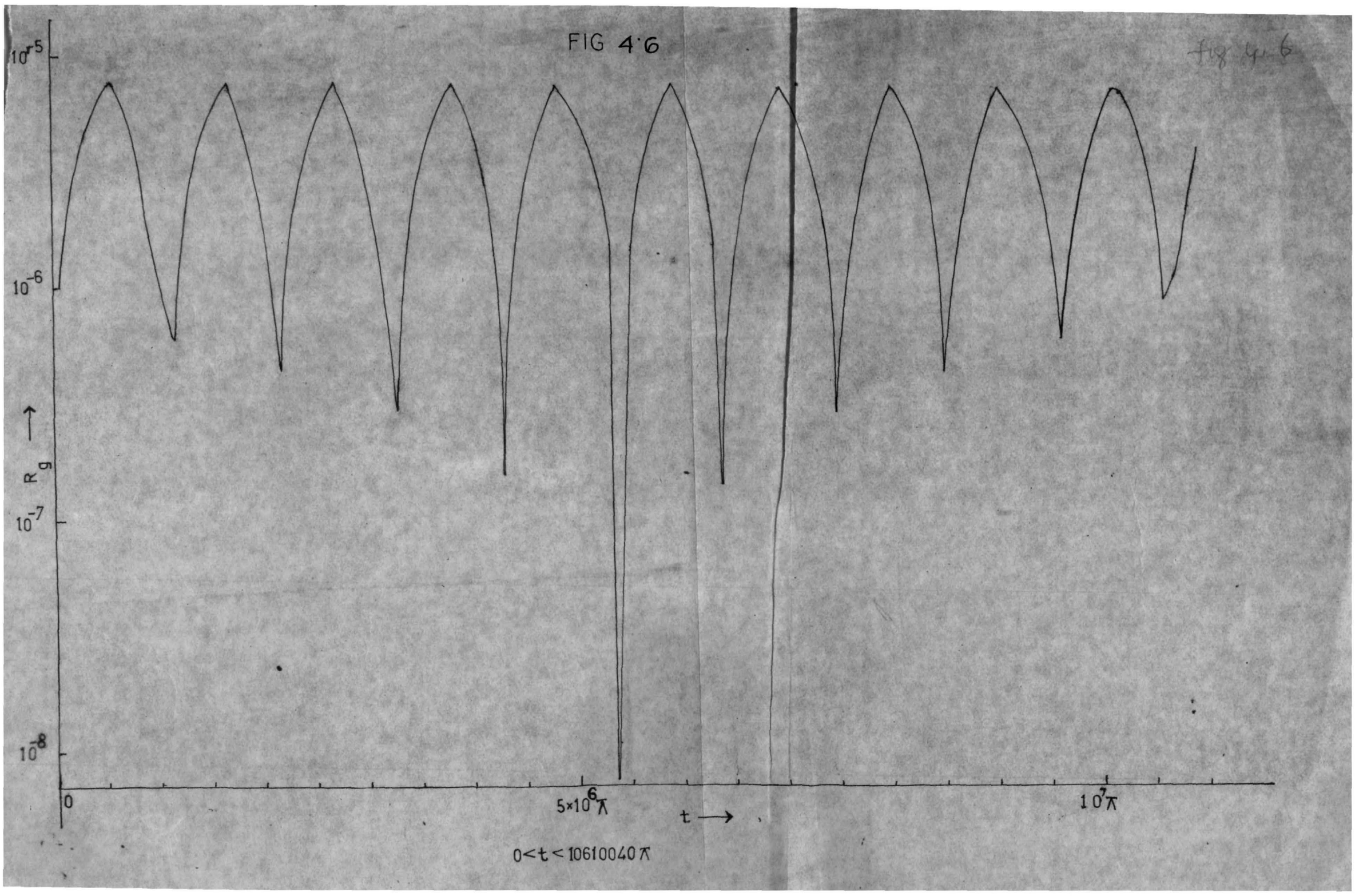

REFERENCES

1. Bambi Hu (1982) - Introduction to real space renormalisation group methods in critical and chaotic phenomenon. Phys. Rep. 91

2. Chrystal. G. (1964) - Text book of Algebra Vol 1 and II. Chelsea Publishing Company.

3. Eckmann - J.P. (1981) - Roads to turbulence in dissipative dynamical systems, Rev. Mod. Phys. 53, 643

4. Joseph Ford (1983) - How random is a coin toss ? Physics Today 36 (4)40.

5. Li, T-Y., and J.A. Yorke (1975) - Am. Math. Mon. 82, 985

6. Lorenz E.N (1963) - J. Atmos. Sci. 20, 130

7. Ott. E. (1981) - Strange attractors and Chaotic Motions of dynamical systems, Rev. Mod. Phys 53, 655.

8. Ruelle, David F. Takens (1971), Commun. Math. Phys 20, 167

9. Scudo, F.M. and James, R. Ziegler (1978) - The golden age of Theoretical Ecology : 1923-1940; Lecture Notes in BioMaths. 22, Springer-Verlag.

10. Stewart, I (1981)- Application to Catastrophe theory to the physical sciences Physica 2D (2) 245

11. Yamaguti, M and Ushiki, S (1981) - Chaos in Numerical analysis of ordinary differential Physica 3D (3) 618.